

Fall 2015

MODIFYING FRACTURE CONDUCTIVITY TESTING PROCEDURES

Kent Blair

Montana Tech of the University of Montana

Follow this and additional works at: http://digitalcommons.mtech.edu/grad_rsch



Part of the [Petroleum Engineering Commons](#)

Recommended Citation

Blair, Kent, "MODIFYING FRACTURE CONDUCTIVITY TESTING PROCEDURES" (2015). *Graduate Theses & Non-Theses*. Paper 60.

This Thesis is brought to you for free and open access by the Student Scholarship at Digital Commons @ Montana Tech. It has been accepted for inclusion in Graduate Theses & Non-Theses by an authorized administrator of Digital Commons @ Montana Tech. For more information, please contact ccote@mtech.edu.

MODIFYING FRACTURE CONDUCTIVITY TESTING PROCEDURES

by

Kent Blair

A thesis submitted in partial fulfillment of the
requirements for the degree of

Master of Science in Petroleum Engineering

Montana Tech

2015



Abstract

Fracture conductivity testing is a measure of how proppant will perform downhole when injected. The current American Petroleum Institute (API) procedure for conductivity testing produces results that are difficult to replicate. In one case three commercial labs tested the same sample of proppant, the results varied between labs and the highest spread in data had an 80% variation (Anderson, 2013). The goal of this thesis is to investigate cell loading procedures that reduce the variation in laboratory results.

A variety of cell loading techniques were tested including Hoke cylinder injection, guar injection, and cell vibration. Hoke cylinder loading was determined not to be a feasible technique with the current lab equipment at Montana Tech's Research Lab.

The guar injection produced a smaller spread in the data when compared to the API loading technique. However, when the results from the guar injection were analyzed it was apparent the guar had not been completely removed from the cell after injection. The remaining guar reduced the overall permeability of the proppant pack, which lead to an unfair comparison with the API Standard procedure.

The cell vibration technique produced conductivity values that were very similar to the results produced by the API procedure but with a considerable reduction in the overall variance.

From the data, it is recommended to test the effect of cell vibration on long-term fracture conductivity tests.

Keywords: Proppant, Conductivity

Dedication

I dedicate this thesis to George Costanza who taught me not to “fly too close to the sun on wings of pastrami.”

Acknowledgements

First I would like to give a huge thank you to Susan and Richard Schrader. Sue was my advisor throughout grad school and has been immensely helpful. Rich is the lab director for the Petroleum department and has taught me how to run a proper fracture conductivity tests. Rich is also a constant source of ideas and solutions when it came to issues about my thesis. I would also like to thank Burt Todd, Brandon DeShaw, and Paul Conrad for being on my thesis committee and generating valuable feedback for me. These five individuals kept me on track and enabled me to complete my thesis on time.

I would also like to thank Carbo Ceramics and Halliburton. Carbo Ceramics generously donated 20/40 ceramic proppant that I used in my thesis testing. Halliburton has donated equipment to Montana Tech and built the Halliburton Research Lab where I conducted my research for this thesis. Without their generous donations, this research would not have been possible.

Table of Contents

ABSTRACT	II
DEDICATION	III
ACKNOWLEDGEMENTS	IV
TABLE OF CONTENTS	V
LIST OF TABLES	VII
LIST OF FIGURES	VIII
LIST OF EQUATIONS	IX
GLOSSARY OF TERMS	X
1. HYDRAULIC FRACTURING	1
2. FRACTURE CONDUCTIVITY LAB TESTING	3
2.1. ISSUES WITH CURRENT PROCEDURE.....	5
2.2. OTHER ISSUES.....	6
3. NEW CELL LOADING TECHNIQUE	8
3.1. HOKE CYLINDER LOADING	9
4. PROPOSED TESTING PROCEDURE	11
4.1. CELL VIBRATION	11
4.2. MODIFIED TESTING PROCEDURE.....	11
5. STATISTICAL ANALYSIS	15
6. SYSTEM	17
7. PROCEDURE AND RESULTS	20

7.1. API TESTING PROCEDURE.....	20
7.2. PROPPANT INJECTION	26
7.2.1. Hoke Cylinder Injection.....	27
7.2.2. Narrow Mouth Wash Bottle Injection	30
7.2.2.1. Guar Mixing and Testing Procedures	32
7.2.2.2. Guar Presence Issue	34
7.2.3. Guar Injection Results	37
7.3. CELL VIBRATION	43
7.3.1. Cell Vibration Procedure.....	43
7.3.2. Cell Vibration Results	45
8. CONCLUSIONS	50
9. RECOMMENDATIONS AND FUTURE RESEARCH.....	51
9.1 FUTURE RESEARCH.....	52
REFERENCES.....	54
APPENDIX A: CONDUCTIVITY RESULTS.....	55
APPENDIX B: RAW DATA.....	57

List of Tables

Table I: Recommended test parameters for high strength proppants (API RP 61, 1989) .13	
Table II : Statistics For Standard API Procedure.....24	
Table III: Permeability Statistics for Standard API Procedure.....26	
Table IV: Hoke Cylinder Injection Results29	
Table V: Guar Concentration Testing.....31	
Table VI: Proppant Mass Injection Testing32	
Table VII: API Standard Loading Procedure and Guar Presence Data Comparison35	
Table VIII: API Standard Loading Procedure and Guar Injection Data Data Comparison39	
Table IX: Standard Procedure and Guar Injection Average Width Comparison.....40	
Table X: Vibration Test44	
Table XI: API Standard Loading and Vibration Data46	
Table XII: API Standard Loading and Vibration Average Widths.....48	

List of Figures

Figure 1: Permeability vs. stress for 16/30 white sand (Barree, et al. 2003)	6
Figure 2: Sandstone Platen Shear Failure	7
Figure 3: Cooke Cell Discrete Element Modeling Simulation	8
Figure 4: 300cc Hoke Cylinder.....	10
Figure 5: API Loading Initial Test.....	22
Figure 6: API Loading Technique Conductivity Graph	23
Figure 7: API Loading Technique Permeability Graph	25
Figure 8: Cell Cross Section	28
Figure 9: Narrow Mouth Wash Bottle Injection	30
Figure 10: Guar Presence Conductivity Graph.....	34
Figure 11: Guar Presence vs API Standard Loading Procedure Permeability Graph.....	36
Figure 12: Guar Injection Conductivity Graph.....	37
Figure 13: API Standard Procedure and Guar Injection Data Spread Comparison	38
Figure 14: API Standard Procedure and Guar Injection Permeability.....	40
Figure 15: Guar Loaded Proppant vs API Standard Loading	41
Figure 16: Loaded Cell Inside Clamps	43
Figure 17: Vibration Conductivity Graph.....	45
Figure 18: Vibration and API Testing Procedure Conductivity Error Graph.....	47
Figure 19: Vibration and API Testing Procedure Permeability Graph.....	49
Figure 20: Barnett shale samples shaped to fit into modified API conductivity cell (Zhang, et al. 2013)	52

List of Equations

Equation(1)	3
Equation(2)	4
Equation(3)	15
Equation(4)	15
Equation(5)	16
Equation(6)	18
Equation(7)	20

Glossary of Terms

Term	Definition
API	American Petroleum Institute: Produces standards for testing in the oil and gas industry
Proppant	Solid material that props open fractures created by a hydraulic fracture treatment
Permeability	How easily a fluid flows through a medium
md	Millidarcy: Permeability units
Conductivity	The product of fracture permeability and propped fracture width
Mean	A calculated central value of a set of numbers
Standard Deviation	A measure that quantifies the amount of variation of a set of data values
Statistical Variance	A measure of how data distributes itself about the mean or expected value
Guar Gum	A polysaccharide when added to water generates high viscosities
Cooke Cell	API 19D Standard testing cell
Hoke Cylinder	Seamless pipe with two threaded ports to allow for connections

1. Hydraulic Fracturing

Hydraulic fracturing (fracking) has become one of the most widely used well stimulation operations in the petroleum industry. With advances in hydraulic fracturing technology, unconventional reservoirs which were previously not economically viable, are now major oil and gas producers.

Hydraulic fracturing is a process where liquid is injected into a well above a formation's fracture pressure and physically splits the formation to form a fracture. Once a fracture (frac) is created, solid particles are injected with fluids downhole to fill in and propagate the fracture. The solids are called proppants. Proppant material can vary, from naturally occurring sand grains to resin coated ceramics. Proppant ensures a fracture does not close once the frac fluid stops pumping.

One indicator of a successful frac is a large fracture conductivity value. Fracture conductivity is the width of the generated fracture multiplied by the permeability of the propped region. The propped fracture has a much higher permeability than the surrounding formation and acts as a high permeability channel for fluids to flow through, which improves production for the well.

To measure how proppant will perform in a frac, API standards have been created. The current standard for long-term fracture conductivity is "Measuring the Long-term Conductivity of Proppants" API RP-19D, 2008. In the presentation "Performance of Fracturing Products" (Anderson, 2013), Anderson explained that labs using the current API standard were experiencing variation between their results and other labs' results by as much as 80%, when "the variations in pack width and permeability show that conductivity variations of $\pm 20\%$ about a mean are within laboratory accuracy for a given proppant type and size" (Barree, et al. 2003).

To have a commercial lab perform long-term conductivity tests on proppant can cost more than \$20,000. With such a high price it is important that tests produce reliable and repeatable results. That is why reducing the variation in long-term conductivity testing is a main focus for researchers.

Montana Tech has a research lab that contains two machines capable of measuring fracture conductivity to API standards; the single cell fracture conductivity system and the dual cell conductivity system. The dual cell system allows two proppant samples to be tested simultaneously, providing the user with an instant comparison of fracture conductivity values between the two samples. Using the dual cell conductivity system to conduct tests, this thesis will focus on reducing variation in fracture conductivity testing.

2. Fracture Conductivity Lab Testing

To simulate a frac in the lab, API standards 61 (1981) and 19D (2008) have been developed to measure conductivity inside a Cooke cell. The cell has a top and bottom piston that applies stresses to simulate formation stress experienced by proppants. Between the pistons and proppant pack are sandstone platens which simulate formation rock. The platens must be 6.95 in to 7 in in length, 1.46 in to 1.5 in wide, and a minimum of 0.35 in thick. Between the platens, proppant is spread out evenly then compressed. The pistons must apply stress at a rate of 100 psi/min \pm 5 psi/min until the cell has reached a 2000 psi increment. Once the appropriate stress has been reached, the cells must be held under this stress for 50 h \pm 2 h. After that period, a 2% by mass KCl fluid is pumped through the cell. The flow rate is 2 ml/min to 8 ml/min to ensure laminar flow is achieved. The minimum pressure drop in the cell must be from 0.002 psi to 0.004 psi. A minimum of five data points must be taken over this range to calculate an average permeability for the corresponding stress. The equation, in SI units used to calculate proppant pack permeability is outlined in API RP-19D (2008), can be seen in Equation 1.

$$k = \frac{\mu QL}{100A(\Delta P)} \quad (1)$$

Where

k is the proppant pack permeability in darcy

μ is the viscosity of the test liquid at room temperature in cp

Q is the flow rate in cm³/s

L is the length between pressure ports in cm

A is the cross-sectional area in cm²

ΔP is the pressure drop ($P_{\text{upstream}} - P_{\text{downstream}}$) in kPa.

To calculate the conductivity, pack widths must also be measured using a digital caliper at each stress. The conductivity equation in SI units defined in API RP-19D (2008) is shown in Equation 2 below.

$$kW_f = \frac{\mu QL}{100w(\Delta P)} \quad (2)$$

Where

k is the proppant pack permeability in darcy,

W_f is the pack thickness in cm,

μ is the viscosity of the test liquid at room temperature in cp,

Q is the flow rate in cm^3/s ,

L is the length between pressure ports in cm,

w is the width of the cell in cm

ΔP is the pressure drop ($P_{\text{upstream}} - P_{\text{downstream}}$) in kPa.

Once an average permeability and pack conductivity have been determined at a specific stress level, the closure stress must then be increased to the next 2000 psi stress interval. This procedure is repeated until the conductivity measurements are taken for each appropriate stress level that a proppant must experience. Natural sands are tested at 2000 psi, 4000 psi and 6000 psi while ceramics are tested at 2000 psi, 4000 psi, 6000 psi, 8000 psi and 10000 psi (API RP-19D, 2008). The conductivity and permeability values identified provide a baseline of how the proppant should perform when exposed to similar stresses in the field.

2.1. Issues with Current Procedure

The procedure detailed in API RP-19D (2008) is set in place to ensure there is consistency in lab conductivity tests. Unfortunately, it has become evident that even with this practice in place there is still a large variation in different labs' results. These labs were testing the same proppant at the specified stress levels and still were unable to produce similar results. There are a variety of explanations for this variance, the method for loading proppant into the cell, is one possible explanation. The current procedure requires the proppant sample to be split into four equal units. The units are poured as evenly as possible into the cell. A leveling device is then used to even out the proppant distribution. With this procedure in place, labs still have difficulties replicating the same results as other labs. The article "Realistic Assessment of Proppant Pack Conductivity for Material Selection" (Barree, et al. 2003), indicates the largest variation in width is caused by the original unstressed packing arrangement. The variation in initial packing conditions also influences the measurement of pack permeability, but to a larger degree. The permeability vs stress graph for 16/30 white sand (Barree, et al. 2003) can be seen in Figure 1.

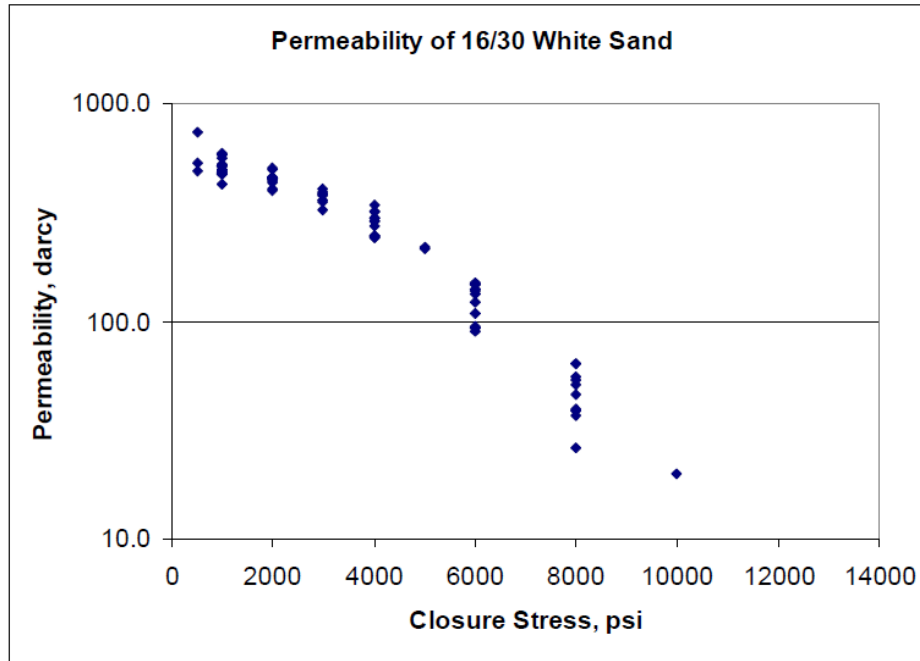


Figure 1: Permeability vs. stress for 16/30 white sand (Barree, et al. 2003)

The graph indicates that the initial pack permeability (at around 500 psi) has much higher variation than measurements taken at 2000 psi and 4000 psi. As the test continues with higher closure stresses, the variation begins to increase at 6000 psi. Reducing the initial pack variation will be one of the main focuses of this thesis. To achieve this new, loading techniques will be investigated.

2.2. Other Issues

In addition to cell loading techniques, sandstone platens used in conductivity tests are another source of variation. In Anderson's presentation (Anderson, 2013), various sandstone platens were subjected to long-term conductivity testing. Once testing had been completed, each platen was photographed. Numerous platens had cracked, stretched and chipped during the testing. There was also evidence that the proppant had embedded in the plates. With these defects present in a large number of the cores, the sandstone fines released from cracking,

embedding, etc. plug pore throats and reduce the conductivity during the test. Developing a new platen design is an area of investigation for future thesis projects.

Piston design is another possible project topic to be investigated. The current piston is causing the cracks to form along the outside of the sandstone platens. This can be seen in Figure 2.



Figure 2: Sandstone Platen Shear Failure

The piston has a rubber O-ring that exerts the majority of the stress along the edges of the core, causing shear failure to occur. Before API RP-19D (2008) was introduced, API RP-61 (1989) was the standard for conductivity measurements. In the original procedure, “the pistons, platen shims, and test chamber should be constructed of 316 stainless steel material” (API RP 61, 1989). Using stainless steel shims drastically reduces embedment and fine releasing during testing, because steel is not as soft as the sandstone. The steel shims can withstand higher stresses than the sandstone which eliminates the tensile failure and edge failure experienced by the sandstone platens. For these reasons the tests run for this thesis will use the API RP 61 (1989) stainless steel shims.

3. New Cell Loading Technique

The cell loading procedure that is proposed in API RP-19D (2008) produces an initial pack which leads to high variation in width and permeability; the main cause of the variation is proppant rearrangement. When a large stress is applied to the proppant pack, the proppant is compressed and begins to shift, which can cause point loading. Point loading occurs when the majority of the stress is applied to a few of the grains instead of the entire pack which causes embedment and crushing. Figure 3 is a simulation conducted that illustrates a cell experiencing point loading (Mattson, et al. 2014).

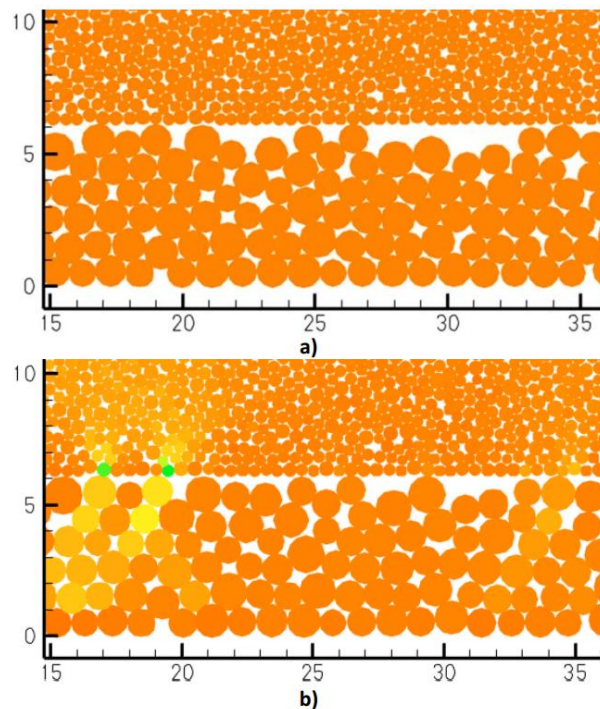


Figure 3: Cooke Cell Discrete Element Modeling Simulation
 a) Initial proppant pack prior to the application of piston displacement b) Final proppant location after compaction and proppant rearrangement.

In the simulation conducted by Mattson, et al. a cell filled with proppant experienced rearrangement once stress was applied. Image a) depicts the cell before loading, where the smaller circles represent the top sandstone platen and the larger circles represent the proppant.

Image b) is the cell under stress, again the smaller circles represent the sandstone platen and the larger circles represent the proppant. The dark orange colour indicates zero vertical stress while the lighter colours indicate regions of stress, where the green is the most stressed area. Only two areas inside the cell experience the majority of the stress, while the bulk of the cell experiences zero vertical stress. This simulation provides strong evidence that point loading occurs inside the cells once stress is applied; a more efficient loading technique would help reduce this effect.

The variations in pack width and permeability show that conductivity variations of $\pm 20\%$ about a mean are within laboratory accuracy for a given proppant type and size (Barree, et al. 2003). With a new loading procedure, the initial pack width and permeability variation should be reduced which will also reduce the overall variation experienced with fracture conductivity analysis testing.

3.1. Hoke Cylinder Loading

The current procedure for cell loading, requires a lab worker to pour in proppant and use a leveling device to ensure the proppant is evenly distributed throughout the cell. Having individuals pack cells ensures there will be variation between different labs' proppant packs. Replacing the individual who personally loads the cell with a mechanical loading procedure should reduce variation. The first proposed change to the loading procedure is the use of a Hoke cylinder, which is shown in Figure 4.

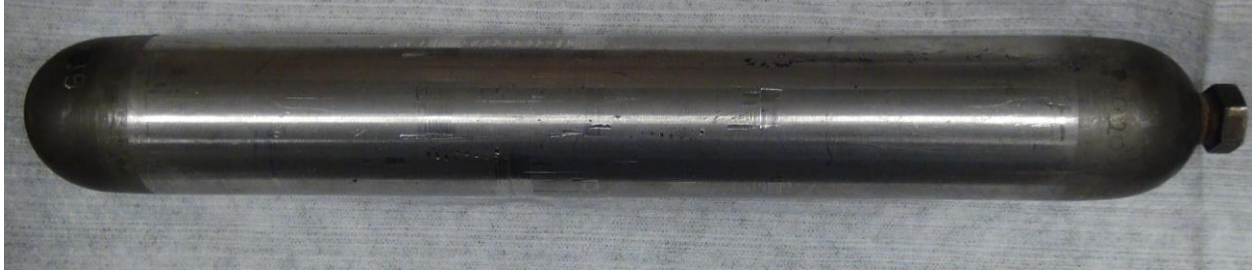


Figure 4: 300cc Hoke Cylinder

A Hoke cylinder is a pressurized vessel, which is capable of injecting proppant into the cell. The cell was properly loaded with shims and platens and then set to a predetermined width. A clamp was set on the pistons to ensure the pistons remain at the specified width while the proppant is injected. The cylinder was filled with proppant, a 2% KCl solution and pressurized with N₂. Tubing with a diameter large enough to flow proppant through, was attached to one end of the cylinder and the other end was attached to the cell. Mesh screens covered every port except the inlet port in the cell, to allow for drainage once the proppant had been completely injected. After all the proppant had been displaced into the cell, testing began.

Wet loading with a Hoke cylinder gives a more realistic representation of how proppant is transported into a formation during a frac where it is pressurized and immersed in liquid. With the proppant immersed in the fluid, the proppant should settle in a semi uniform arrangement. Mesh screens were placed on all the ports to ensure the injected liquid is removed from the cell but the proppant remains. The use of a Hoke cylinder should produce more repeatable results and help to reduce the overall variation experienced in fracture conductivity tests.

4. Proposed Testing Procedure

To test the new loading techniques discussed in this thesis, a modification to the current API RP-19D (2008) procedure will have to be made due to time constraints since the long-term conductivity tests take a minimum 150 hours to complete. The test will be run on each loading procedure to evaluate which technique produces the least variation.

4.1. Cell Vibration

Another area of investigation is the use of low amplitude vibration on loaded cells before testing. In sand pack experiments where data consistency is essential, vibration is used to create tight packs. Sand is split into samples and slowly poured into a cylindrical sand pack holder which is constantly experiencing vibration. The sand is then allowed to compact under the vibration before adding more sand. By adding the remaining samples to the container a tight sand pack is formed. This use of vibration can be applied to cells to develop a tighter pack for the proppant.

Currently API RP-19D (2008) states “The proppant shall not be packed by vibration or tamping, as this can cause segregation of material.” (API RP-19D, 2008). With natural sand proppant vibration can cause the separation of grain size, the larger grains will sink to the bottom and the smaller grains tend to stay on top of the pack. The CARBOLITE ceramic proppant chosen to be used in these experiments have very little grain size difference, so when exposed to vibration there should be minimal grain segregation which makes this proppant a promising candidate for cell vibration.

4.2. Modified Testing Procedure

The proppant will be tested using the dual cell conductivity system where both cells will be loaded using the same technique and will be run simultaneously. The dual cell system

provides an instant comparison between the two Cooke cells and allows the user to measure the variation in conductivity. The proppant used in testing will be a 20/40 ceramic, a synthetically made ceramic proppant in which all the samples are almost identical in size. This will produce a much tighter pack and eliminate conductivity reductions due to proppant failure. The alternative to using a ceramic is a natural sand proppant which varies in size and sphericity and is more prone to crushing. After each test, proppant samples will be replaced to avoid failures due to fatigue. API RP-19D (2008) requires an initial stress of 50 psi on the cell once the proppant is loaded, then the closure stress is increased to 500 psi. The pistons then apply each necessary closure stress with a ramp rate of 100 psi/min. During the testing the cell will be heated to 250 °F to meet API requirements for synthetic proppants.

As discussed previously, due to time restrictions each loading procedure will not be tested at each closure stress for the recommended 50 hour period. The proppant will be tested at closure stresses for the length of time recommended in API RP 61 (1989), short-term conductivity testing. By minimizing the variables that change, from short-term to long-term testing, the result will provide a better indication of how successful the loading technique is in producing a repeatable conductivity value. The conductivity values produced using API RP 61 (1989) guidelines should be much higher than the long-term conductivity because the system will not reach steady state in that time period, but this will allow for more testing to be conducted on various loading techniques. For this thesis a minimum of eight short-term conductivity tests using numerous loading techniques were tested. The results were compared to see if new loading techniques were able to produce results with less variation than the API standard loading procedure. The long-term conductivity tests are the industry standard but if long-term tests were conducted the number of test run would be significantly lower. With fewer tests run it would be

difficult to make comparisons between various loading techniques. For these reasons, having more data for various loading procedures was deemed more important than running fewer of the industry standard long-term conductivity tests.

Table I indicates the specified closure stresses, flow rates and testing times for high strength proppants from API RP-61 (1989) short-term conductivity testing. The highlighted values will be applied in testing as part of this thesis.

Table I: Recommended test parameters for high strength proppants (API RP 61, 1989)

Closure Stress (psi)	Flow Rates (cm ³ /minute)			Time at Stress (hour)
1000	2.5	5	10	0.25
2000	2.5	5	10	0.25
4000	2.5	5	10	0.25
6000	2.5	5	10	0.25
8000	2.5	5	10	0.25
10000	2.5	5	10	0.25
12000	2.5	5	10	0.25
14000	2.5	5	10	0.25

For these tests, proppant will be tested at pressures up to and including 8000 psi- since the CARBOLITE proppant used in testing is crush rated for 10,000 psi. This means that at 10,000 psi the proppant begins to fail due to crushing and more than 10% of the total proppant has been crushed to fines smaller than the 40 mesh. To minimize the variation in results due to proppant crushing and releasing fines, the proppant will only be tested to 8000 psi. Each stress will be applied to the cell for the appropriate 0.25 hours (15 minutes). The flow rates used in the experiment will be modified from API RP-19D (2008). The three rates controlled by the mass flow controller used in Montana Tech's Research Lab are 2 cm³/min, 4 cm³/min, and 8 cm³/min. Another change to the short-term procedure is the test fluid. Distilled water is recommended in API RP-61(1989), but to better replicate the long-term parameters a 2% KCl solution will be

used. In long-term testing the 2% KCl is used over the distilled water to eliminate clay swelling in the sandstone platens. The clay swelling is not an issue with the tests run for this thesis since the sandstone platens were substituted with more reliable steel platens. Even with the change in platen material, the 2% KCl is used as the test fluid to reduce the amount of variables that change and contribute to variation when switching from short-term to long-term tests. Using the data collected, statistical analysis will be performed to determine the variation for each method.

5. Statistical Analysis

The average conductivity at each stress or the mean conductivity is the first step in statistical analysis which is calculated using Equation 3

$$\bar{x} = \frac{\sum x}{n} \quad (3)$$

Where

\bar{x} is the mean

x is the conductivity values

n is the number of samples

After the mean is determined, the standard deviation is calculated with Equation 4

$$s = \sqrt{\frac{\sum (x - \bar{x})^2}{n - 1}} \quad (4)$$

Where

s is the standard deviation

x is the conductivity values

\bar{x} is the mean

n is the number of samples

The sample standard deviation is a measure of variation of all values from the mean (Triola, 2006)- a large standard deviation indicates there is a large spread in the data. The final variable is variance which is a measure of how far the data is from the mean. Variance is calculated using Equation 5.

$$\text{Sample Variance} = s^2 \quad (5)$$

where

s^2 is the standard deviation squared.

In the paper Realistic Assessment of Proppant Pack Conductivity for Material Selection (Barree, et al. 2003), the authors determined that $\pm 20\%$ in conductivity variations are within lab accuracy. With these newly proposed procedures the goal is to produce variations of less than $\pm 20\%$.

6. System

The system used for testing is the dual cell press located in Montana Tech's Petroleum Engineering research lab. In this system, two prepared cells are placed on top of each other and set inside the load frame. In the base of the frame is a 100 ton hydraulic piston. The piston is filled with pressurized oil from a syringe pump located below and is able to move the two cells up into a static steel slab. As the piston pushes the cells further into the steel slab, the cells experience a greater closure stress.

The first stress the cells are exposed to is 50 psi. At this stress, connections for the differential pressure transducers, pressure gauges, silica saturation vessels and outlet ports can be made without the cells moving.

The silica saturation vessels are Hoke cylinders filled with silica which the 2% KCl flows through before entering the cells. The vessels help reduce the degradation of proppant and platens and help to remove solids.

After the cells are connected, the heating bands and vessel heaters are plugged in. For the heating bands a thermocouple must be placed inside the cell body to monitor the temperature. The silica saturation vessels each have a thermocouple beneath the heating bands and are both covered in glass insulation wrap for safety. Once all the devices' thermocouples are secured and their heating sources are plugged in, a two zone heater is used to slowly heat the system to 250 °F.

Once the system reaches the API specified 250 °F for proppant testing, pressurized nitrogen is used to fill the bladder accumulators which contain the 2% KCl solution. The bladder expands and moves the fluid into the cells which generates an internal pressure of 400 psi. The internal pressure chosen for these tests was 400 psi which is the median value for the API

recommended range. As the fluid flows through the cells the internal pressure increases, the hydraulic piston compensates for the change in internal pressure by moving upward to ensure the designated closure stress is applied to the cells.

The internal pressure of the cells are measured with a differential pressure transducer. The pressure transducer is connected to the high end (the port closest to the silica saturation vessels) and the low end (the port closest to the outlet of the cell). The transducer has an internal membrane which measures the deflection from the high and low ends and reports the differences as a pressure. The differential pressure transducer used is a Remanufactured Rosemount® and is capable of measuring drops as low as 0.0001 psi.

The cells are then pressurized to the target stress where a telescoping gauge is used to measure the gap width on all four corners of the cell. Equation 6 is used to calculate the width of the pack.

$$\textit{Pack Width} = \textit{Measured Gap Width} - \textit{Zero Gap Width} \quad (6)$$

The zero gap width is a measure of a cell's gap without any proppant in the cell at every stress level. When proppant is tested the, zero gap width is subtracted from the measured gap width to give the actual width of the proppant pack. The average pack width for each cell is used to calculate the conductivity.

For the all tests conducted in this thesis the standard sandstone shim was replaced with a steel shim. This eliminates fines release due to embedment and shim failure during testing.

To measure the conductivity or permeability for each cell a mass flow controller is used to maintain a constant flow rate. One cell at a time diverts its flow to the mass flow controller. Initially the mass flow is closed which causes the entire system to stop flowing. With no flow the pressure transducers will eventually measure a zero pressure drop through the cell. After this

condition is met the mass flow began to flow $2.00 \text{ cm}^3/\text{min}$. Three flow rates are conducted at each closure stress and the pressure drop at each flow rate is recorded. This process continues up to and including the final closure stress of 8000 psi.

Over the course of performing all of the conductivity tests, two mass flow controls were used. The first mass flow control used was designed to operate at $70 \text{ }^\circ\text{F}$. But after running numerous tests where the fluid is heated to $250 \text{ }^\circ\text{F}$ the mass flow control eventually stopped working. The valve was stuck fully open and was unable to close. After replacing the initial mass flow with a new device rated to $150 \text{ }^\circ\text{F}$ the system ran for a few more tests without issues but eventually the new mass flow began having problems due to the high operating temperatures. For future tests it is recommended that the mass flow controllers be switched out with a new controller that is rated for higher temperatures or the fluid should be cooled before entering the mass flow controller.

The remaining variables for calculating the permeability and conductivity for the pack are constants. The viscosity for a 2% KCl solution is taken from Table C.1 in API 61 (1989), at $250 \text{ }^\circ\text{F}$ the 2% KCl has a viscosity of 0.248 cp. The length is the measurement from the high end pressure port to the low end which is 12.7 cm. The area is width of the cell which is 3.835 cm multiplied by the width of the pack.

For each closure stress the average of the three calculated permeabilities and conductivities are taken and plotted against closure stresses.

7. Procedure and Results

As proposed, multiple techniques were tested for this project. This included the standard API testing procedure, using a Hoke cylinder to inject proppant, wet loading proppant, and cell vibration. CARBO Ceramics generously donated their CARBOLITE ceramic proppant which was used in every test. To measure the applicability for each procedure a total of 31 fracture conductivity tests were run and analyzed.

7.1. API Testing Procedure

As discussed previously the API procedure for loading proppant into a cell produced the data to which all other procedures' data will be compared. The amount of proppant used in each test was calculated using Equation 7.

$$W_p = (41\text{cm}^3)\rho \quad (7)$$

Where

W_p is the weight of the proppant in grams

ρ is the bulk density of the proppant in g/cm^3 .

This equation calculates the mass of proppant required to produce a 0.25 in pack inside the cell which is the recommended width in API 61 (1989). The CARBOLITE proppant used in testing, has a bulk density of 1.55 g/cm^3 , therefore the mass of proppant used in each test was 63.55 g.

The cells were first prepared by placing a lubricated O-ring around the ridge on the bottom piston. The piston was then inserted into the cell and locked into place using four set screws along the base of the cell. Next, the bottom platen was lowered into the cell onto the piston with the testing face upward. The platen was placed just below all 5 ports in the cell. When the platen was placed in the cell, 100 mesh screens were placed in each port to prevent

proppant from leaving the cell during testing. Room Temperature Vulcanized Silicone (RTV) sealant was then applied around the edge of the bottom platen and cell wall. Any excess RTV was removed from the face of the platen and the sealant was allowed to dry for at least 12 hours. A razor blade was used to remove any remaining RTV from the cell wall. The heating band was then placed on the outside of the cell and tightened using two nuts on the back of the bands. With the band connected to the cell, the pressure fittings were placed into the five ports in each cell.

A proppant mass of 63.55 g was measured out. This sample was then split into four samples, each with a mass of 15.888 g. Each sample was poured into the cell. Then, using a caliper with a steel plate the proppant was leveled out inside the cell. The top steel platen was placed into the cell with the test side facing down. RTV was again applied to the outside of the platen and left to dry. The top piston with another lubricated O-ring was inserted into the top of the cell but was not secured. The completed cell was placed with another cell into the hydraulic load frame and tested.

A total of 10 fracture conductivity tests were run to measure the variability in the API standard cell loading procedure. Data from the first four tests are plotted in Figure 5.

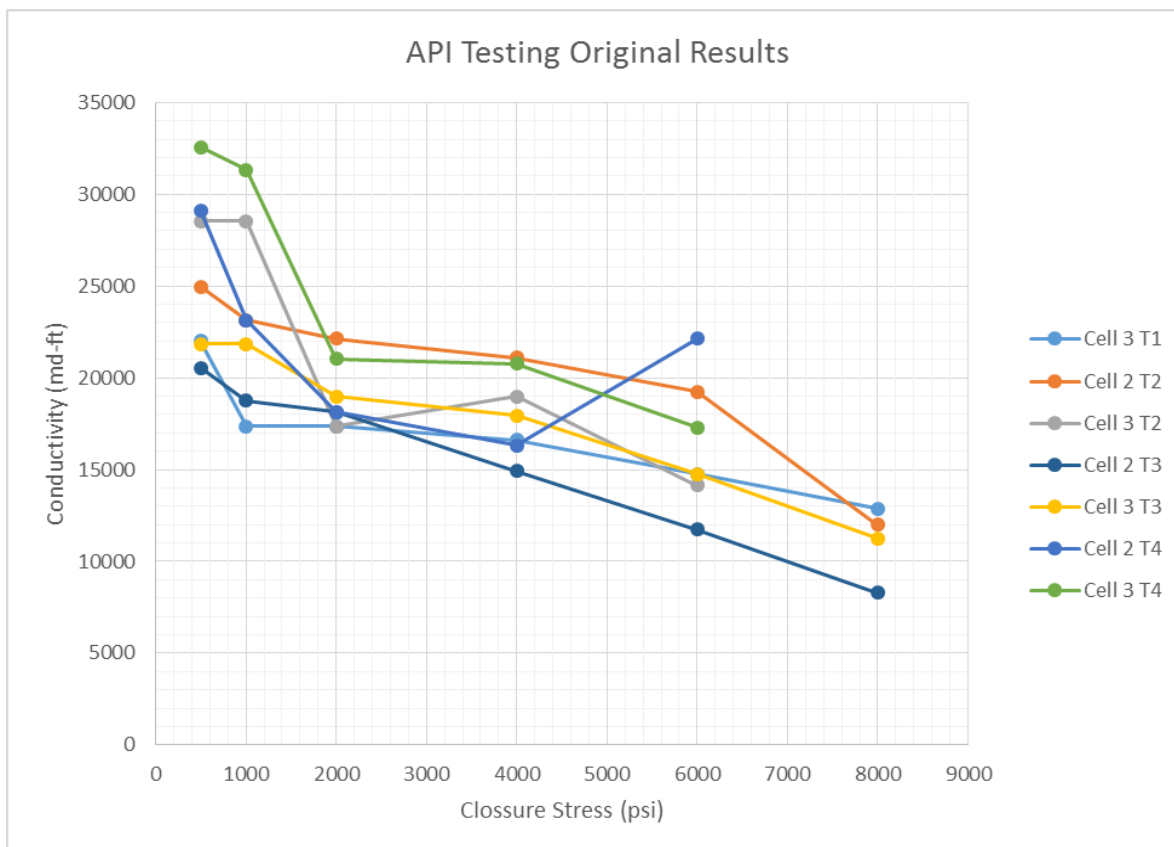


Figure 5: API Loading Initial Test

The first four tests produced results with error in the data. For Cell 2 Test 4 there were massive variations in the pressure transducer readings. Once the pressure stabilized the measured drop was extremely low causing the conductivity from 4000 psi to 6000 psi to increase dramatically. This was due to the pressure transducers, which needed to be cleaned and then zeroed. Due to the fluctuating pressure, Test 4 was ended at 6000 psi for both Cell 2 and Cell 3. For Cell 2 Test 1 and Cell 3 Test 2, the 20 mesh screens used to keep the proppant in the cells, but allow fluid through, became plugged at the high end pressure port. The plugging was likely caused by the silicon sealant used on the outside of the interior shim. With a plugged high end port, the pressure transducer measured a very large negative value since only one half of the

transducer was experiencing a pressure. Due to the plugging issues, Cell 2 Test 1 and Cell 3 Test 2 were invalid and discarded.

The data set indicates a large variation for conductivity measurements at 500 psi and 1000 psi closure stresses. Initial variation was expected as other labs were also experiencing a large range of conductivity at these stresses, but not to this extent. As more tests were conducted with other procedures, it became evident that there was an aspect of human error involved with this initial data set. At this stage, cell preparation and system operation were at their weakest condition. By running more tests, cell widths began to vary less and tighter conductivity spreads began to develop for other procedures. Another five tests were run using the API standard loading procedure, to help remove human error. The results of the new tests are shown in Figure 6.

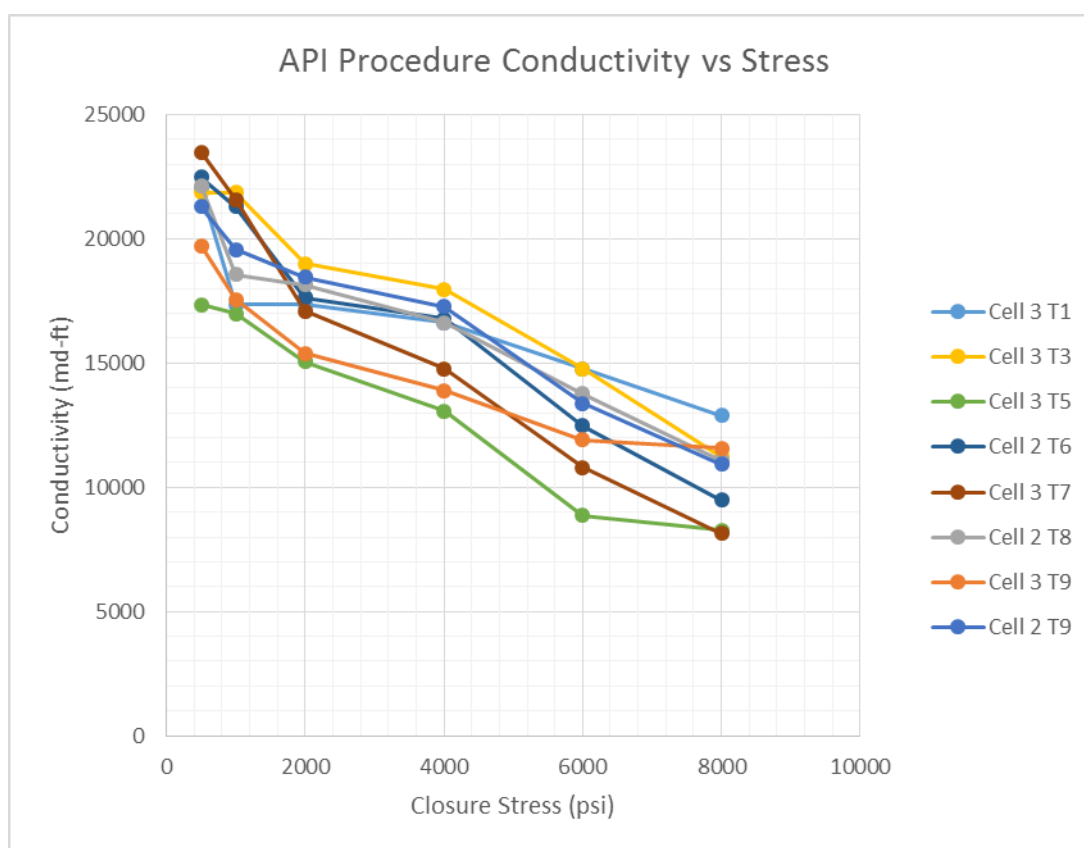


Figure 6: API Loading Technique Conductivity Graph

The new tests produced significantly better results with the API standard loading procedures. The initial data had conductivities ranging from 21,000 md-ft to 33,000 md-ft at a closure stress of 500 psi whereas the new data conductivities ranged from 17,000 md-ft to 24,000 md-ft at 500 psi. This newly acquired data tested all cells to 8000 psi. At 6000 psi and 8000 psi there was less variation in the data compared to the old set. With better results the second set of data is referenced for comparison for the remainder of this thesis.

For the data set, seven conductivity test results were used to calculate the statistics which can be seen in Table II.

Table II : Statistics For Standard API Procedure

Closure Stress (psi)	Average Conductivity (md-ft)	Standard Deviation	Variance
500	21,633	2507	6,285,704
1000	19,811	2277	5,186,623
2000	17,700	2357	5,554,122
4000	16,214	2671	7,133,495
6000	12,915	3246	10,536,238
8000	10,208	1575	2,480,842

The data highlights that at low closure stresses the variance was high, but at 6000 psi the variance was the highest and at 8000 psi the variance was the lowest. The causes of high variation in the data include fines releasing, proppant rearrangement, embedment, and point loading (Barree, et al. 2003). The API standard tests were conducted using steel shims and ceramic proppant. With these modifications embedment and fines releasing should be drastically reduced or eliminated. The data therefore indicates that the current cell loading procedure which produces a fluffy proppant pack experienced major proppant rearrangement when exposed to initial closure stresses. One explanation for the large reduction in variance from 6000 psi to 8000 psi could be at 6000 psi the proppant was still undergoing rearrangement inside the cell. At

8000 psi the proppant pack was compressed to the point where movement inside the cell was limited. This was the maximum bulk density of the pack before grain failures begin to occur. With minimized movement, the conductivity values calculated at this stress varied the least compared to conductivities calculated at all other closure stress levels.

The permeability calculated using the API standard procedure follows the same trend as the conductivities. This is plotted in Figure 7.

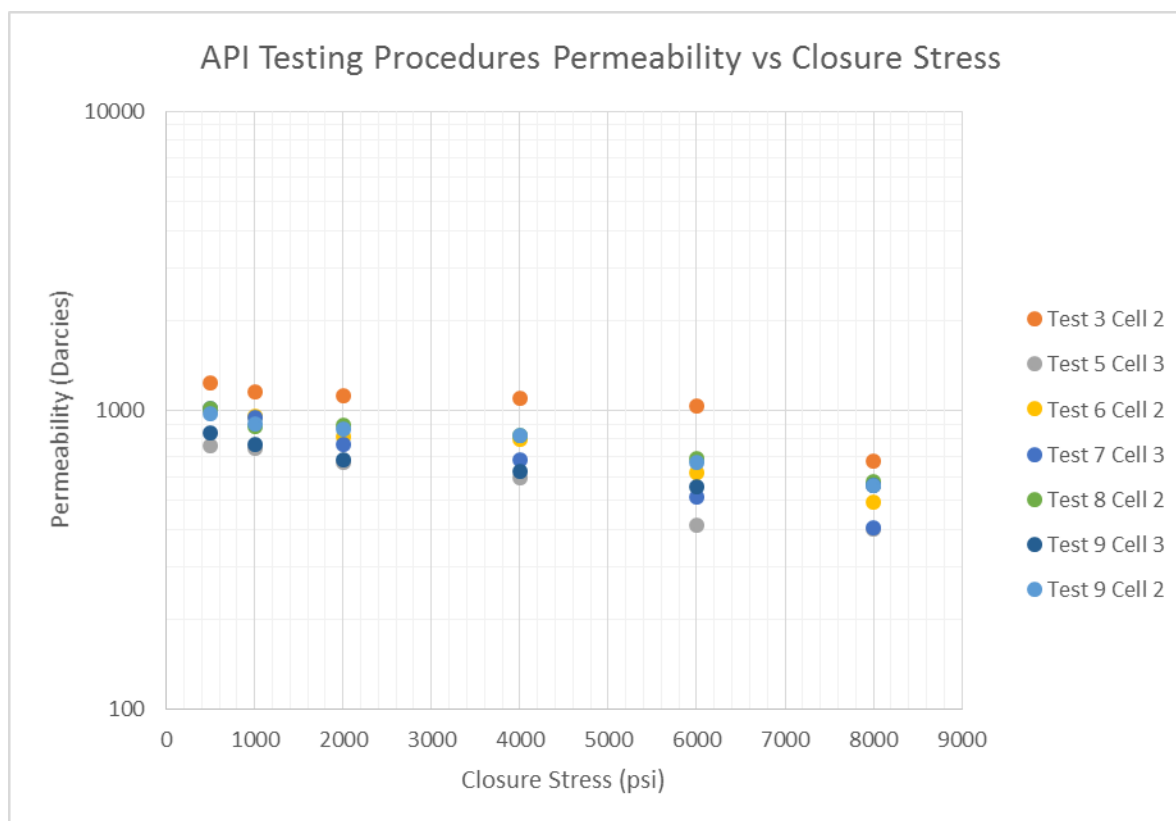


Figure 7: API Loading Technique Permeability Graph

Comparing these results to the permeability vs closure stress graph from the article *Realistic Assessment of Proppant Pack Conductivity for Material Selection* (Barree, et al. 2003) there is a definite trend. The authors determined that if the initial permeability had a high level of variance, then at higher closure stresses the variance will be even larger. Figure 7 has a large spread for the permeability at the initial closure stress of 500 psi, but as closure stress increases

to 4000 psi and 6000 psi the data shows the largest spread in results. The permeability statistics for the API standard procedure are shown in Table III.

Table III: Permeability Statistics for Standard API Procedure

Closure Stress (psi)	Average Permeability (Darcies)	Standard Deviation	Variance
500	978	150	22,471
1000	909	136	18,629
2000	830	154	23,621
4000	779	168	28,386
6000	641	198	39,251
8000	524	100	9,956

The calculated variance at 500 psi was considerably larger than the variance at 1000 psi. From Realistic Assessment of Proppant Pack Conductivity for Material Selection (Barree, et al. 2003), with this high initial variance it is expected that at higher closure stresses the variance will be much greater. Comparing this statement to the calculated data, this is true except for the final closure stress. At 8000 psi the variance is the lowest amongst all the closure stresses. The main difference between these test results and the article results is the proppant. The 20/40 ceramic proppant tested in this thesis had a crush resistance of 10,000 psi, where the 16/30 White Sand used in the article had a crush resistance of around 4000 psi. At 6000 psi and 8000 psi the White Sand experienced major proppant crushing and fines release, both of which are attributed to spreads in the data. The 20/40 ceramic proppant at 6000 psi and 8000 psi were still being compressed into a pack and very few of the proppants experience failure.

7.2. Proppant Injection

Removing the variation due to individuals leveling packs was a major focus for this project. Instead of the standard API loading procedure where samples were split and evenly

poured into the cells and then leveled, multiple methods were tested for the capability of injecting proppant into a cell.

7.2.1. Hoke Cylinder Injection

The first technique tested was the use of a Hoke cylinder to inject proppant into the cells to simulate how proppant is transported during an actual hydraulic fracture process. To be able to test the validity of injecting the proppant, the API standard procedure for cell preparation needed to be modified.

The cell's bottom piston was locked into the proper position with set screws and the bottom platen was secured to the cell with RTV. Mesh screens were placed in every port except the inlet which permitted proppant to flow into the cell. To determine the proper amount of proppant to be injected into the cell, a 0.25 in gap between the top and bottom platen needed to be introduced. This was achieved by using a digital caliper to measure 0.25 in from the bottom platen, then the thickness of the top platen was added to get a total overall height.

The cell was then turned on its side, with pressure ports facing down to eliminate the chance of screens falling out. The gap measurement was then marked in numerous locations inside the cell. The sides of the top platen were thoroughly coated in RTV. Any RTV that spread onto the face of the platen was cleaned off immediately. Two screws were then inserted into the drilled and threaded holes that partially penetrate the steel shims. The shims were then slowly and evenly lowered into the cell until the top of the platen was flush with the gap measurements marked on the cell. RTV was then spread around the top platen to ensure a proper seal. Once the sealant was dried a razor blade was used to remove any excess RTV on the cell wall. The cells were then placed upright and both heating bands were attached. A digital caliper was used to measure the distance from the top platen to top edge of the cell. This distance was marked

several times on the top piston. The top piston was then inserted into the cell and compressed until the top edge of the cell was even with the marked line on the piston. This ensured that the top piston did not dislodge the top platen when inserting the piston into the cell. A cross section of a constructed cell with a 0.25 in gap is shown in Figure 8.

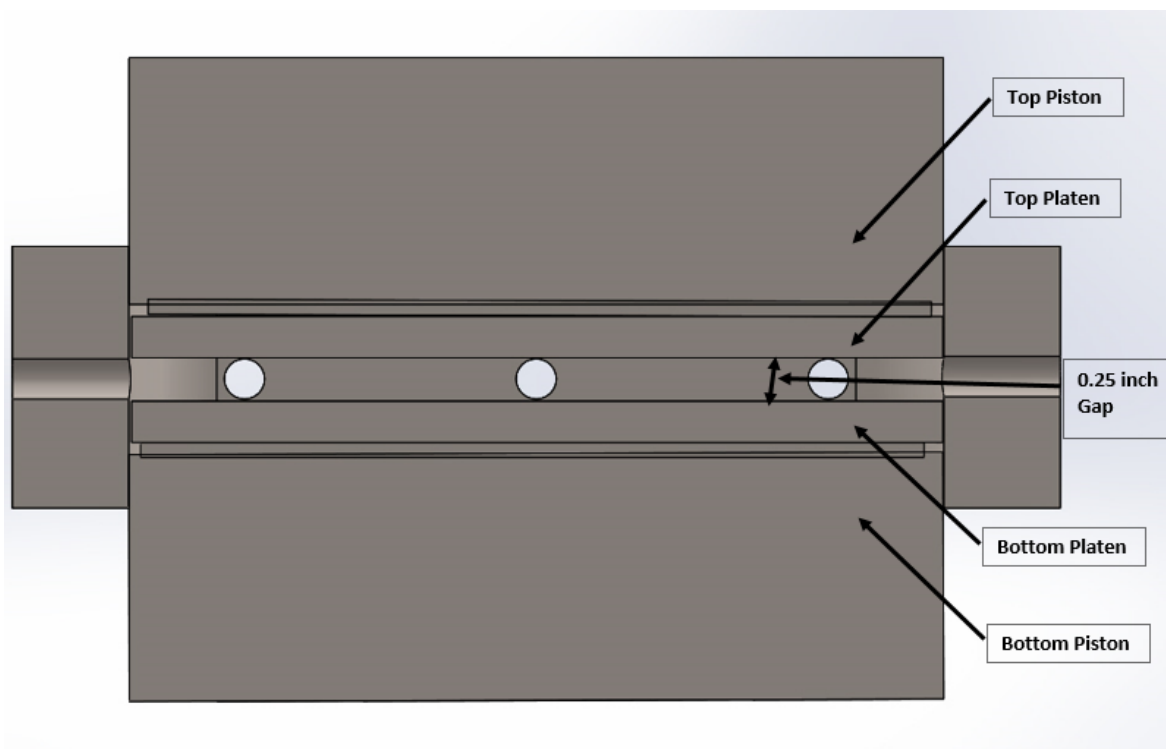


Figure 8: Cell Cross Section

Once the cell was properly constructed caps were placed on all of the pressure ports and tubing was attached to the outlet valve. The cell was then placed in custom-made steel clamps manufactured to fit the cells with 0.25 in of proppant inside. The clamps were also used to ensure that once fluid and proppant were injected into the cell, the mobile top piston was not displaced out of the cell.

When the cell was firmly placed inside the clamps the Hoke cylinder was connected. The front end of the cylinder had a valve with a short piece of tubing connected to the cell. The other

end of the cylinder had another valve with tubing which was connected to a nitrogen tank which was used to pressurize the vessel.

The results of the cylinder loading testing can be seen in Table IV.

Table IV: Hoke Cylinder Injection Results

Test	Solution	Volume (mL)	Displaced mass (g)	Non-Displaced Mass (g)
100g Proppant @ 100 psi	2% KCl	300	6.43	93.57
100g Proppant @ 200 psi	2% KCl	300	10.09	89.1
100g Proppant @ 200 psi	Guar	300	9.14	90.86

Table IV lists the results of the three main tests conducted using a Hoke Cylinder to inject the proppant. Initially when 2% KCl was used to transport the proppant as a slurry, with 300 ml of 2% KCl at 100 psi only 6.43 g out of the 100 g proppant was successfully displaced into the cell. When the pressure increased to 200 psi using the same slurry, only 10.09 g out of the 100 g were displaced. The KCl did not keep the proppant suspended inside the cylinder and when opened to the cell very little proppant was carried.

To increase the viscosity of the injection fluid guar was added to the solution. Guar is a water soluble natural polymer which is used in hydraulic fracturing. When mixed with water the guar drastically increases the viscosity and suspension time for the proppant. This allows for more proppant to stay suspended in solution and be transferred into the fracture. For the final Hoke Cylinder injection test a viscous guar solution was used. When the cylinder was pressurized and opened to the cell only 9.14 g out of 100 g of proppant were transported.

The issue with this process was due to the fittings and tubing that connected the cylinder to the cell. The fittings and 0.25 in outside diameter tubing instantly plugged up when the proppant slurry entered. Due to the lack of availability of larger fittings and tubing and the high

cost of purchasing larger tubing and fittings, this method was rejected in favor of a narrow mouth wash bottle injector.

7.2.2. Narrow Mouth Wash Bottle Injection

During the Hoke cylinder testing, a slurry of guar and proppant was transferred into the cylinder. To move the proppant into the Hoke cylinder a narrow mouth wash bottle was used and the proppant and guar flowed easily through the nozzle. This was the origin of the bottle injector.

The injector consists of a narrow mouth wash bottle with a nut and ferrule attached to the end of the nozzle to enable a connection to the cell. For this test the same cell preparation strategy that was used for the Hoke cylinder was employed. Figure 9 is an image of the narrow mouth wash bottle connected to the cell.

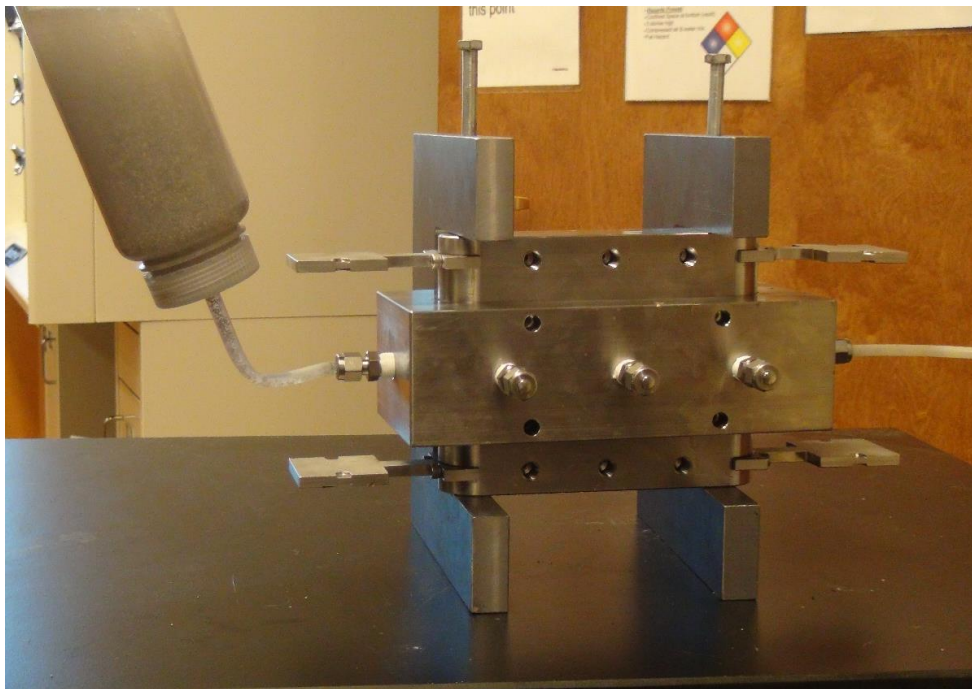


Figure 9: Narrow Mouth Wash Bottle Injection

The cell was capped and placed in the clamps to ensure that the top piston remains static.
(NOTE: This cell is a newly acquired cell which does not have the piston port fittings or caps

attached. If tests were conducted on the cell there will be leakages.) The cylinder was filled with proppant and guar and the outlet port was connected to a vacuum. Initially, the bottle was left to flow without aid which led to very low displacement. Without the ability to pressurize this vessel a vacuum was used to help increase the flowrate.

For this process 2% KCl was unable to keep the proppant in solution which lead to very short proppant settling times. The test results to determine the proper guar concentration are shown in Table V.

Table V: Guar Concentration Testing

Mass Guar (g)	Temperature (°C)	Volume Water (mL)	Result
3	40	300	Too viscous to flow properly
3	40	600	Proppant settling quickly
3	40	450	Proppant settling quickly
3	40	400	Majority of proppant injects

Every batch of guar had 90 g of proppant and was attached to a cell. The first test with 1% guar plugged the nozzle quickly and struggled to flow into the cell. Diluting the guar to a 0.5% concentration, the proppant began settling and displacement was minimal. Using a 0.75% guar solution yielded the best result as the proppant began plugging the nozzle only after the cell had been filled. The results of the tests that were run to determine the mass of proppant needed to fill the cell with the API designated 63.55 g is shown in Table VI.

Table VI: Proppant Mass Injection Testing

Test	Solution	Volume (mL)	Displaced mass (g)	Non-Displaced Mass (g)
90g Proppant	2% KCl	300	14.73	75.27
80g Proppant	0.75% Guar	500	52.66	26.24
95g Proppant	0.75% Guar	480	63.92	31.08
90g Proppant	0.75% Guar	480	64.17	24.83
85g Proppant	0.75% Guar	480	63.8	21.2

For each test more proppant than the API-specified 63.55 g was used because the proppant had a tendency to clog near the outlet port of the bottle and would not flow into the cell. Excess proppant was used to ensure that at least the required 63.55 g of proppant would inject into the cell. The first test run with the 2% KCl solution indicated that a more viscous fluid was necessary to keep the proppant suspended during injection to have a better displacement ratio. The best result was with a 0.75% guar solution and 85 g of proppant which was able to transport 75% of the proppant into the cell resulting in 25% excess proppant. This combination displaced 63.8 g of proppant which was the nearest to the API recommended 63.55 g. The tests which used 90 g and 95 g were able to inject the desired 63.55 g but resulted in more excess proppant.

7.2.2.1. Guar Mixing and Testing Procedures

It was necessary to ensure that all the guar was mixed completely with the water. A standard laboratory Hamilton mixer introduced too much air into the solution. Standard laboratory stir bars were unable to agitate the mixture sufficiently once the majority of the guar had been added to the water. To ensure proper mixing a Carter Motor mixer was used. When connected to a variable transformer the Carter Motor was able to completely mix the proppant without creating a large vortex and introducing air into solution.

The guar preparation procedure was as follows. 3.6 g of guar were measured into a pour boat. 480 mL of water were measured in a plastic container, and 85 g of proppant was measured in another pour boat. The motor's shaft was raised and the plastic container was placed below it. The blade was lowered to 0.5 in above the bottom of the container. The variable transformer was turned until the shaft began to spin. The guar was slowly poured into the container with caution to not spill on the shaft or sides of the container. The variable transformer voltage was slowly increased while adding the guar. At no point should globules of guar form in the solution. If globules did form, the voltage on the transformer was increased until the globule was dispersed into the solution. This process was continued until all the guar was mixed with water. When the solution was completely mixed, proppant was then slowly added while mixing continued for a minute.

After the solution was thoroughly mixed, the fluid and proppant were transferred into the narrow mouth wash bottle. The bottle was constantly agitated to keep the proppant suspended. The bottle was then connected to the prepared cell, all caps were tightened on the ports, and a Welch 1400 vacuum pump was attached to the outlet port. The vacuum was turned on for four to five minutes. Eventually the cell was filled with proppant, and proppant began to build up inside the spray bottle nozzle. Once the proppant in the nozzle became static, the bottle was disconnected and a cap was placed on the inlet port. The vacuum ran for another two minutes to remove excess guar. After two minutes the vacuum and caps were removed from the cell and the cell was taken out of the clamps. This procedure was repeated again for the second cell.

When both cells were filled, they were stacked inside the hydraulic load frame. Then stress was applied to the cells until the cells were static. Then the fittings were attached. With all the fittings connected 2% KCl was flowed through the system to remove any remaining guar

from the cell. Initially the pressure drop inside the cell was quite sporadic due to the guar leaving the cell. Once the pressure drop remained stable inside the cell the guar had been removed. The cells were then heated to the API standard 250 °F and testing begun.

7.2.2.2. Guar Presence Issue

Through the process of determining the plausibility of loading cells with guar and proppant, a few cells failed during the injection process. This left one fully injected cell and one collapsed cell. The fully injected cell was set into the hydraulic press while the collapsed cell was remade. Due to curing times with the sealant the fully loaded cells sat overnight and allowed guar to mix with the proppant. The graphical data in Figure 10 illustrates the effects that guar had on cells without having 2% KCl solution flowed through the cells after injection.

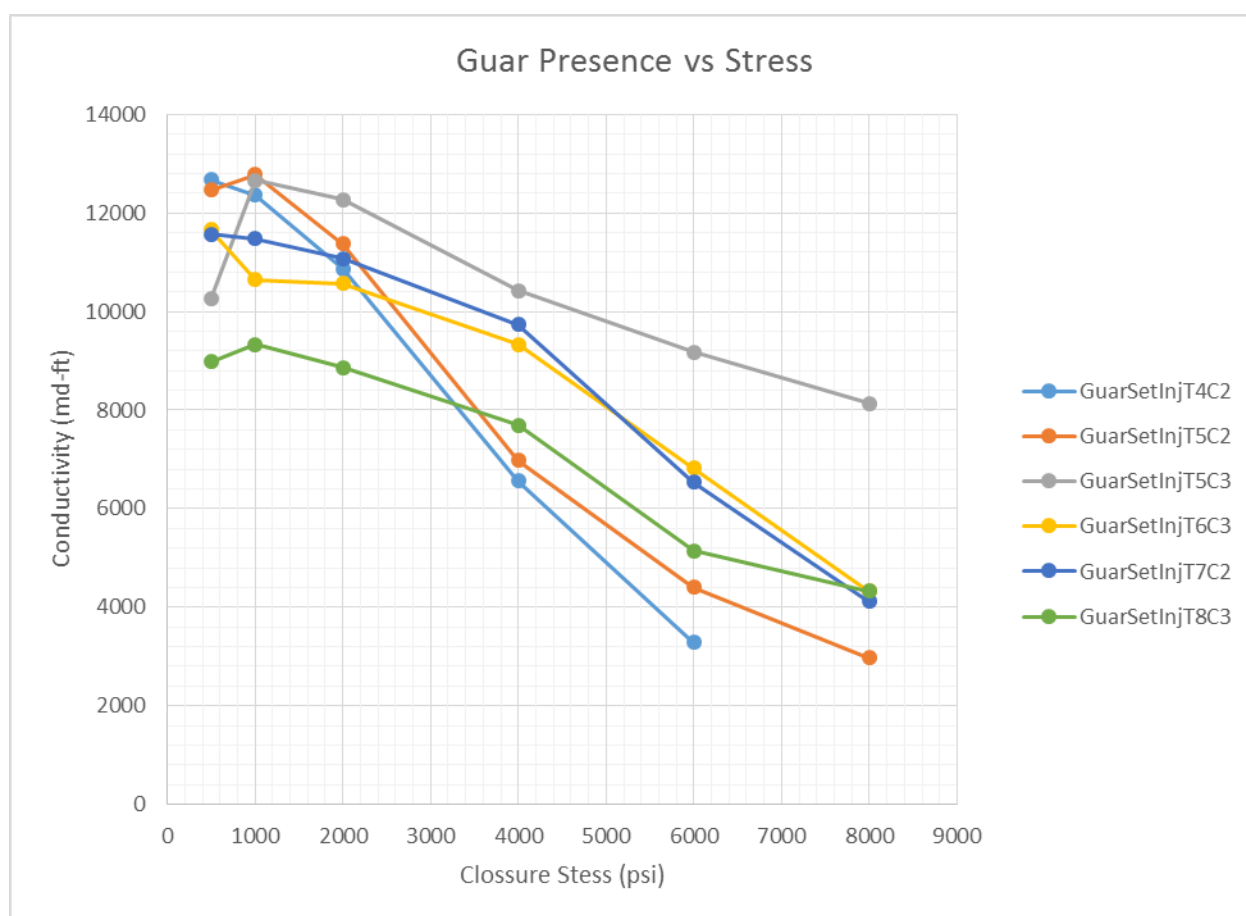


Figure 10: Guar Presence Conductivity Graph

From this graph it is clear that the guar drastically reduced the overall conductivity, when compared to the data collected with the API standard loading procedure. The results of this test showed that after 6000 psi, the data spread was not drastically reduced at the final closure stress. For Test 4 Cell 2 the test was stopped at 6000 psi due to a cell leak which was caused by a fatigued O-ring. With a leak in a cell it is difficult to take readings with the differential pressure transducer. The pressure drop does not remain static for a long enough period of time to take a measurement, instead fluctuating between positive and negative values, thus bringing an early end to the test.

A comparison between the guar set data and the API standard loading procedure data is displayed in Table VII.

Table VII: API Standard Loading Procedure and Guar Presence Data Comparison

API Standard Loading Procedure				Guar Presence Injection			
Closure Stress (psi)	Average Conductivity (md-ft)	Standard Deviation	Variance	Closure Stress (psi)	Average Conductivity (md-ft)	Standard Deviation	Variance
500	21,633	2507	6,285,704	500	11,269	1410	1,986,911
1000	19,811	2277	5,186,623	1000	11,545	1356	1,839,742
2000	17,700	2357	5,554,122	2000	10,837	1130	1,277,179
4000	16,214	2671	7,133,495	4000	8,454	1589	2,523,691
6000	12,915	3246	10,536,238	6000	5,895	2077	4,315,884
8000	10,208	1575	2,480,842	8000	5,199	2038	4,153,955

The average conductivity from the guar set injection on average was 7500 md-ft lower than the API test procedure data. This was a result of the guar coating the proppant and creating more solid packs with lower permeabilities. The guar data also had a much smaller spread in data which was evidenced by the significantly lower variances at every closure stress. Although the variance was much lower for the guar set injection the highest variance was still experienced at the 6000 psi closure stress. Overall when comparing these results, it is evident that the guar influenced the proppant.

Figure 11 is a plotted comparison of the API standard loading procedure and the guar set injection permeability data.

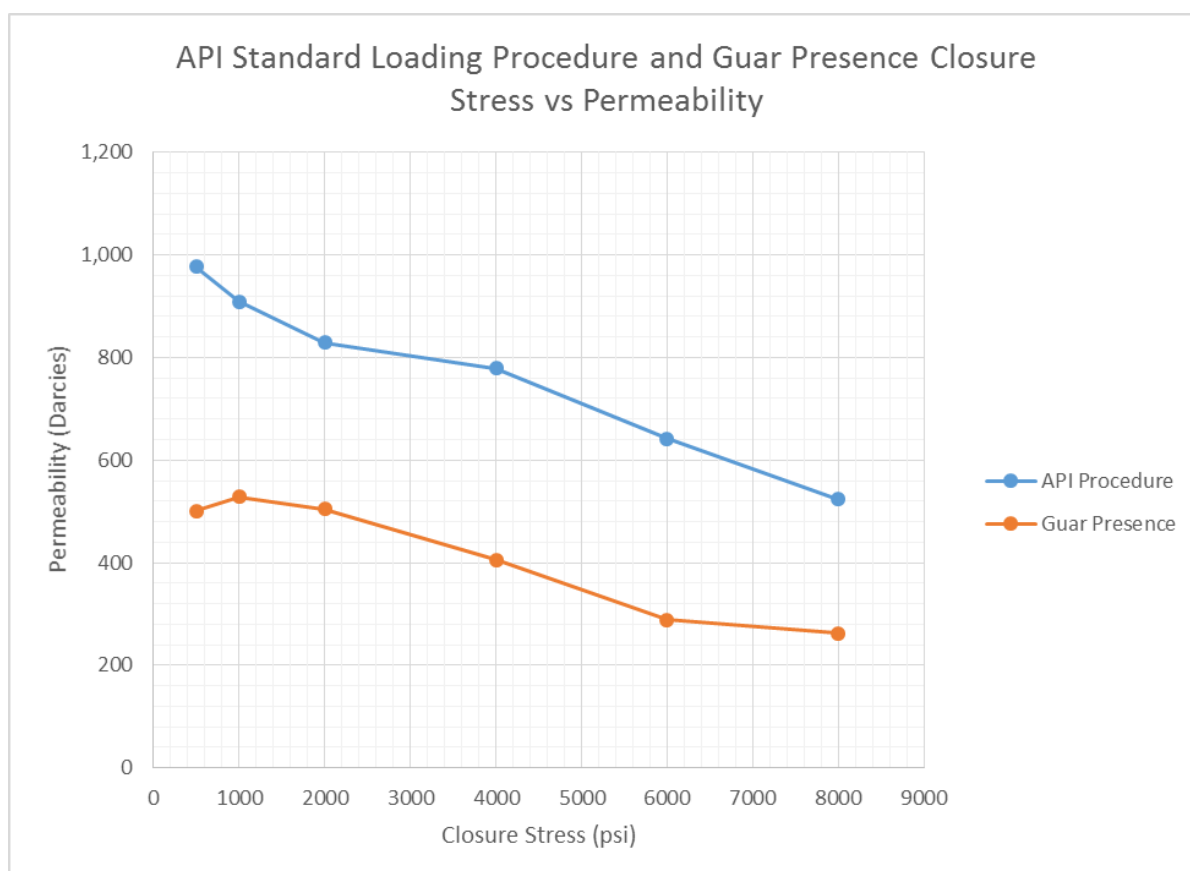


Figure 11: Guar Presence vs API Standard Loading Procedure Permeability Graph

The guar injection permeabilities were substantially lower than those produced by the API standard loading procedure. As the closure stress increased from 500 psi to 1000 psi the permeability increased for the guar injected proppant, which is counter intuitive. As stress is applied, proppant packs become more compacted, reducing the flow area. With a smaller flow area, a higher pressure drop is required to reach the 2.00 cm³/min, 4.00 cm³/min, and 8.00 cm³/min flow rates. With a higher pressure drop a lower permeability is calculated. For the guar set injection to have an increase in permeability from 500 psi to 1000 psi there must be restrictions in the cell to cause a higher pressure drop at 500 psi. While testing the guar set

injection cells, 2% KCl was not introduced into the cells until at least 12 hours after the guar was injected allowing the guar to mix with the proppant. The heated 2% KCl was able to remove some of the guar at 500 psi, but due to the guar being exposed to the 250 °F longer, the pack experiencing a higher stress, and flowing more 2% KCl through the system; more of the guar was removed at 1000 psi closure stress resulting in a higher permeability.

From this data it is evident the guar must be flushed out of the system once the cells are injected with the guar and proppant slurry. The cells must immediately be flushed with 2% KCl to have a fair comparison to the API standard loading procedure.

7.2.3. Guar Injection Results

The guar injection process transports the proppant into the cell where the proppant is naturally arranged. The results from the guar injection test are show in Figure 12.

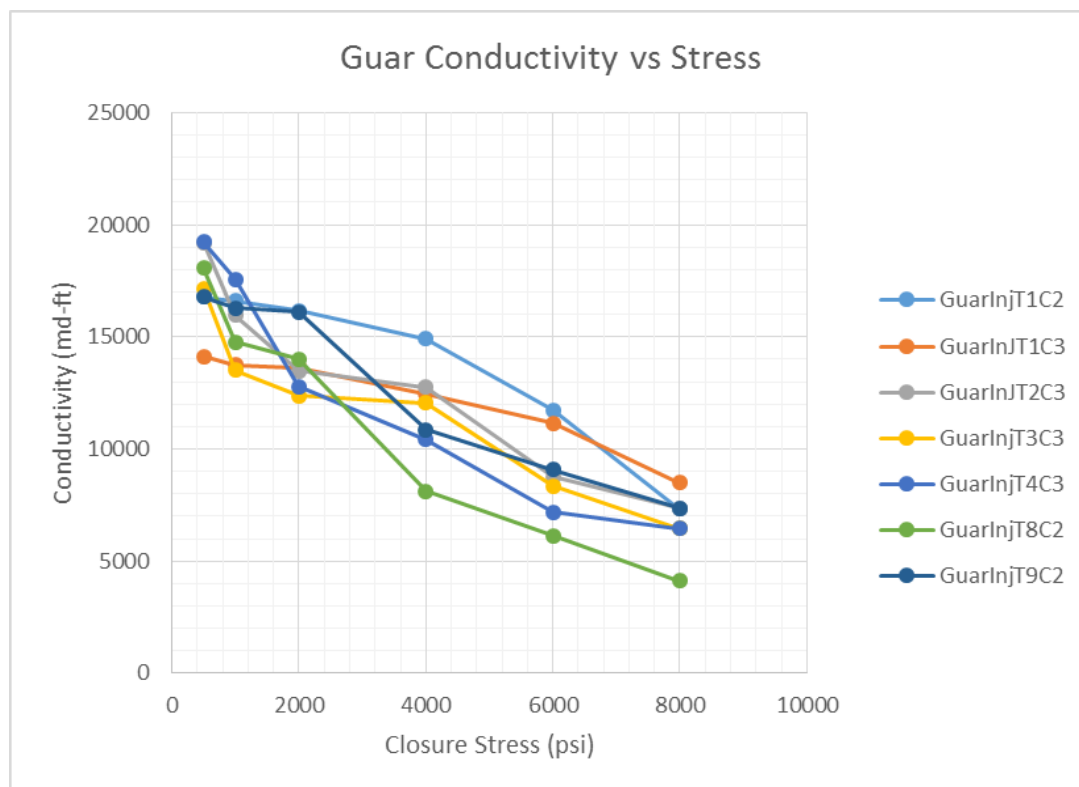


Figure 12: Guar Injection Conductivity Graph

From this graph it is evident that the injection process produces a small spread of conductivity values at the initial closure stresses. As the closure stress increased the injected proppant pack had the same trend as the API loading technique pack. The largest spread in conductivity values occurred at 4000 psi and 6000 psi. At 8000 psi the conductivity spread was considerably reduced which was the same reduction that the API pack experienced. The proppant pack at 6000 psi was very tight. Once the 8000 psi stress was applied there was very little proppant migration, which leads to a small variation in conductivity.

Figure 13 is a comparison between the variance in API testing and guar injection testing.

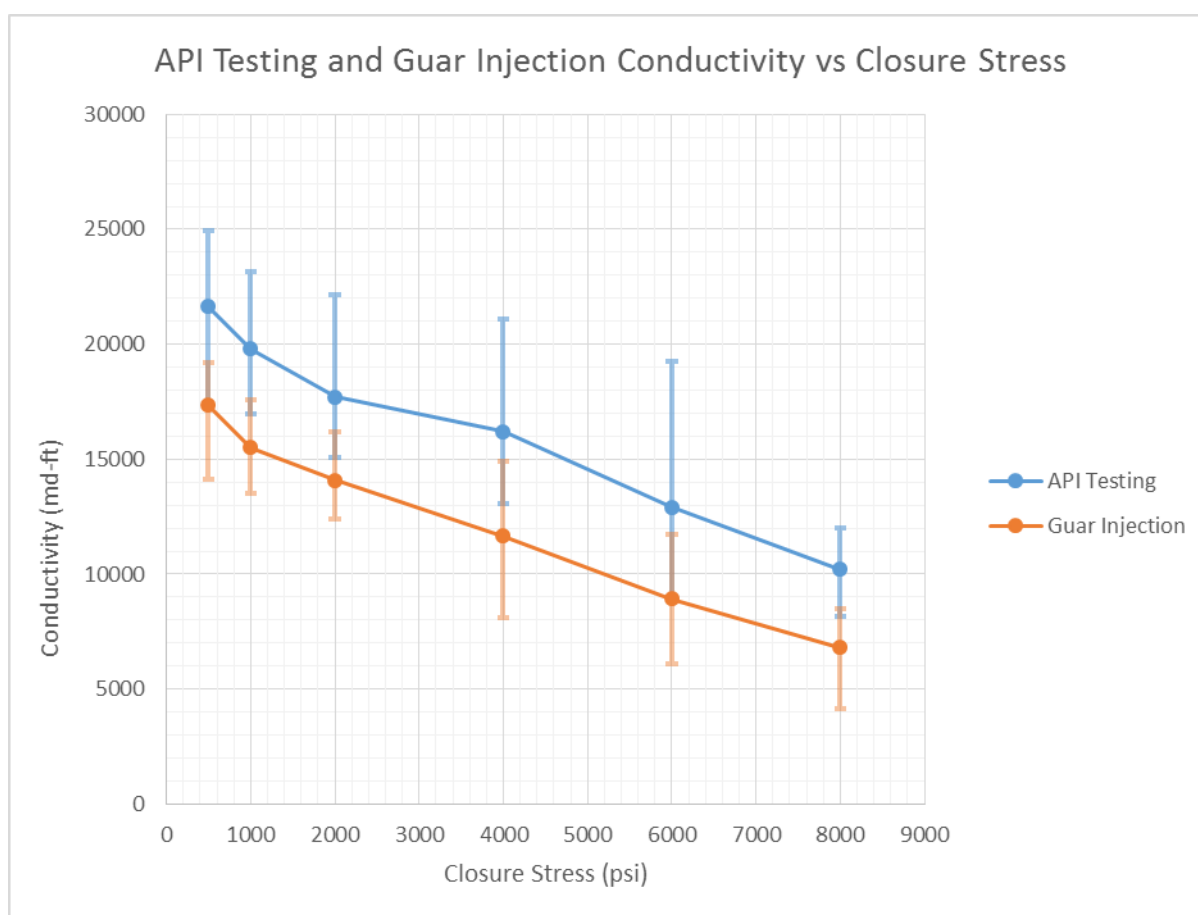


Figure 13: API Standard Procedure and Guar Injection Data Spread Comparison

The blue line represents the spread of conductivity values at each closure stress for the API standard loading procedure. The orange line represents the spread in conductivity values at each closure stress for the guar injection procedure. At every closure stress the guar injection has a smaller spread in data than the standard API procedure results. The calculated data for these results are seen in Table VIII.

Table VIII: API Standard Loading Procedure and Guar Injection Data Comparison

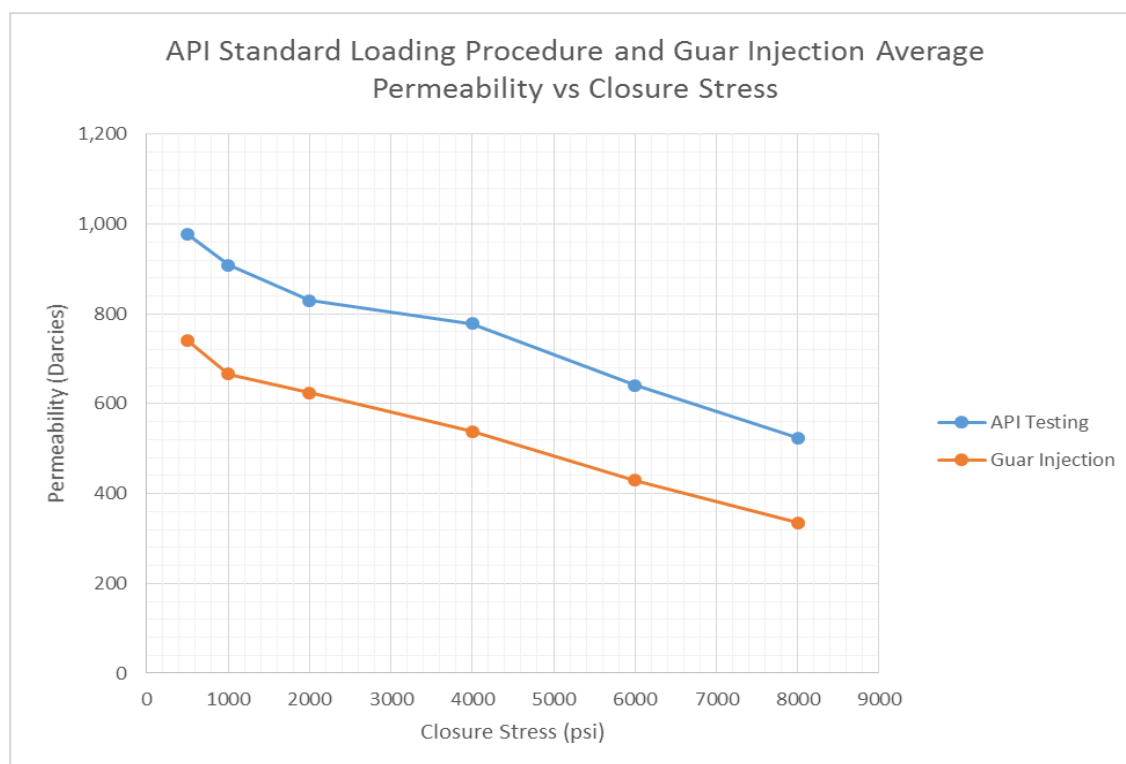
API Standard Loading Procedure				Guar Injection			
Closure Stress (psi)	Average Conductivity (md-ft)	Standard Deviation	Variance	Closure Stress (psi)	Average Conductivity (md-ft)	Standard Deviation	Variance
500	21,633	2507	6,285,704	500	17,336	1,754	3,076,297
1000	19,811	2277	5,186,623	1000	15,495	1,516	2,297,338
2000	17,700	2357	5,554,122	2000	14,082	1,512	2,285,321
4000	16,214	2671	7,133,495	4000	11,657	2,132	4,547,537
6000	12,915	3246	10,536,238	6000	8,911	2,004	4,017,986
8000	10,208	1575	2,480,842	8000	6,796	1,364	1,859,794

The left side of Table VIII is a duplicate of the left side of Table VII, which presents the average conductivity, standard deviation, and variance for the API standard loading procedure results at each closure stress. The right side of Table VIII is the average conductivity, standard deviation and variance for the guar injection. The graph from Figure 13 illustrates that the guar injection had a much lower spread in conductivity values. Table VIII shows how much lower the spread was. On average, the guar injection procedure produces conductivities with half the amount of variance compared to the API standard loading procedure. Although the spread is much lower for guar injection it is interesting to compare the average conductivities for these two tests. The guar injection on average had a 4000 md-ft lower average conductivity than the API standard loading procedure. There are two reasons for the decrease for the guar injection, either the average pack height or a significantly lower permeability. Table IX is a comparison of the average pack height for each test.

Table IX: Standard Procedure and Guar Injection Average Width Comparison

API Standard Procedure		Guar Injection	
Closure Stress (psi)	Average Width (in)	Closure Stress (psi)	Average Width (in)
500	0.2669	500	0.2826
1000	0.2629	1000	0.2808
2000	0.2580	2000	0.2736
4000	0.2520	4000	0.2598
6000	0.2447	6000	0.2491
8000	0.2354	8000	0.2429

Comparing these results, guar injection produced higher average pack widths than API standard loading procedure. On average the guar injection packs were 0.0115 in larger than the API procedure. The differences in the pack widths did not account for the major reduction in conductivity. Figure 14 is a graph of the average permeability for both the API standard procedure and the guar injection.

**Figure 14: API Standard Procedure and Guar Injection Permeability**

From this graph it is clear that the guar permeability is significantly lower at every closure stress. This reduction is not due to packing efficiency, but is caused by non-displaced guar in the cell reducing the overall permeability of the proppant pack. Figure 15 is a comparison between proppant loaded by guar injection and API standard loading procedure under 10X magnification.

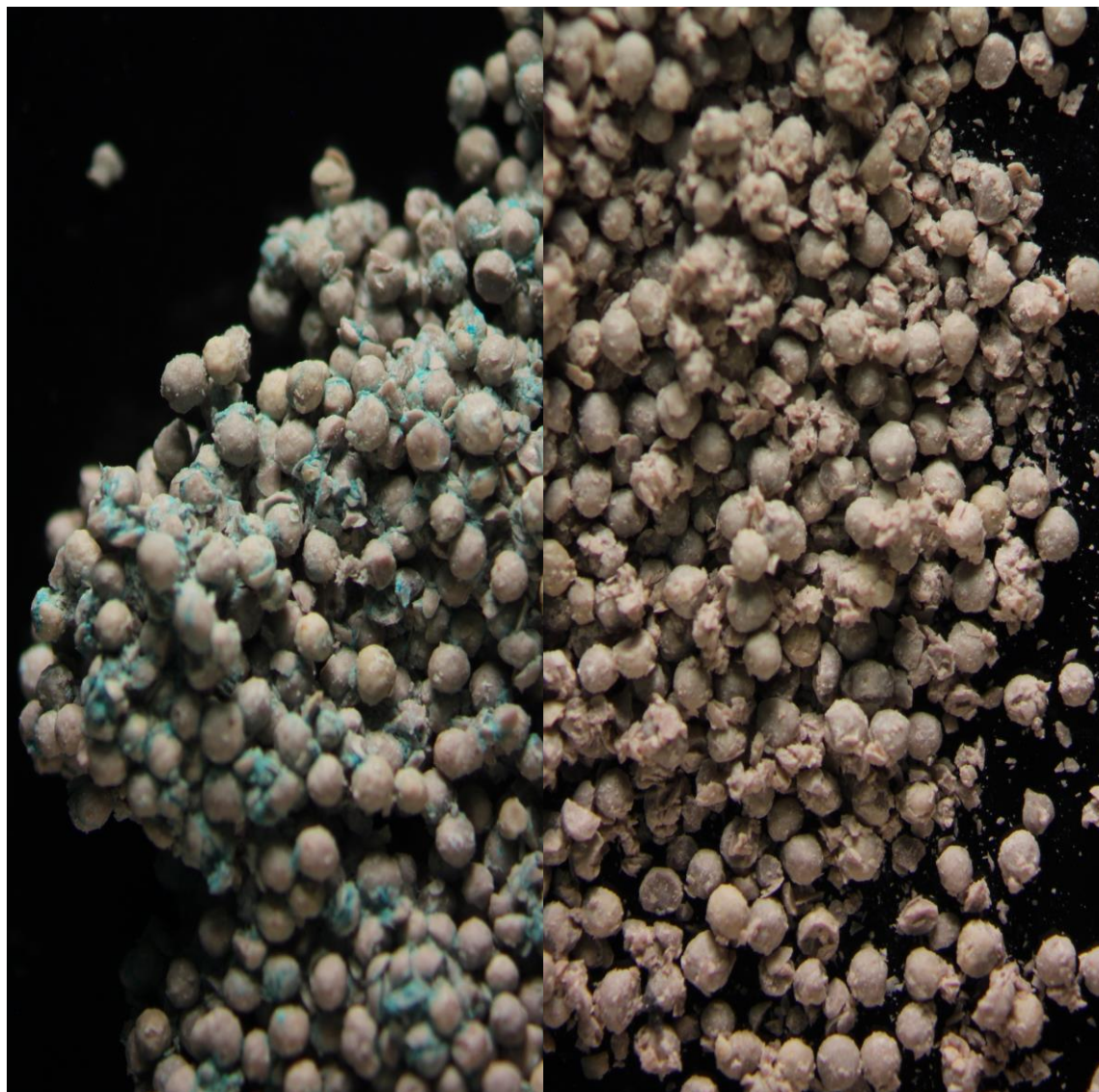


Figure 15: Guar Loaded Proppant vs API Standard Loading

Although loaded differently both samples of proppant were tested up to and including 8000 psi. After the test, the samples were removed from the cells and analyzed at 10X magnification.

The image on the right is a picture of the proppant loaded using API hand loading techniques. There were numerous individual proppant which were unattached to the main mass of proppant. The main mass of proppant was loosely stacked. The image on the left shows proppant loaded using the guar injection technique. The guar was dyed blue so it was easily identifiable. These proppant were in big groups and there were little to no loose grains of proppant. The guar caused individual pieces of proppant to adhere to each other which clogged the pore throats.

With the guar's reduction to the permeability, it is not correct to compare the guar injection data to the API standard loading procedure data. Flushing the cells with the 2% KCl after injection removes some of the residual guar and increases the permeability. This reduction in permeability caused by the inability to remove the injected guar is a realistic issue in actual hydraulic fracturing. Once the fracture fluid and proppant are injected into the formation there is a flow back period where the majority of fracture fluid is displaced out of the reservoir and brought to surface. It is very difficult to recapture all of the fracture fluid and if guar is used there can be reductions in the conductivity caused by the guar plugging pore throats. In long-term testing the residual guar may yield more realistic conductivity values. For this thesis where the goal is to compare various loading techniques and reduce laboratory variation between results, the guar presence in the cells leads to an unfair comparison between procedures.

The API standard is a good evaluation of how the proppant performs under various closure stresses. The guar injection tests produce results with much lower variance. However, with the guar lowering the proppant permeability this testing procedure is not a reasonable evaluation of the proppant.

7.3. Cell Vibration

In API-19D (2008) it states the cell is not to be packed by vibration as this can cause segregation of material. The CARBOLITE proppant tested for this thesis was chosen for its uniform size and sphericity. By using a manufactured ceramic proppant the grain size segregation experienced with vibration is greatly reduced. In sand pack testing to achieve tight packs a vibration table or magnetic vibrator is used to rearrange the sand into a more ideal packing shape. With this addition to the procedure, the results become more repeatable. The impacts of cell vibration on results are discussed below

7.3.1. Cell Vibration Procedure

The cells were prepared using the API-19D (2008) cell building procedure. The cell was then placed inside the manufactured clamps. For these tests a hole was drilled and threaded in each of the clamps to allow a bolt to be thread through the clamp. Figure 16 is a picture of a prepared cell inside the clamps.

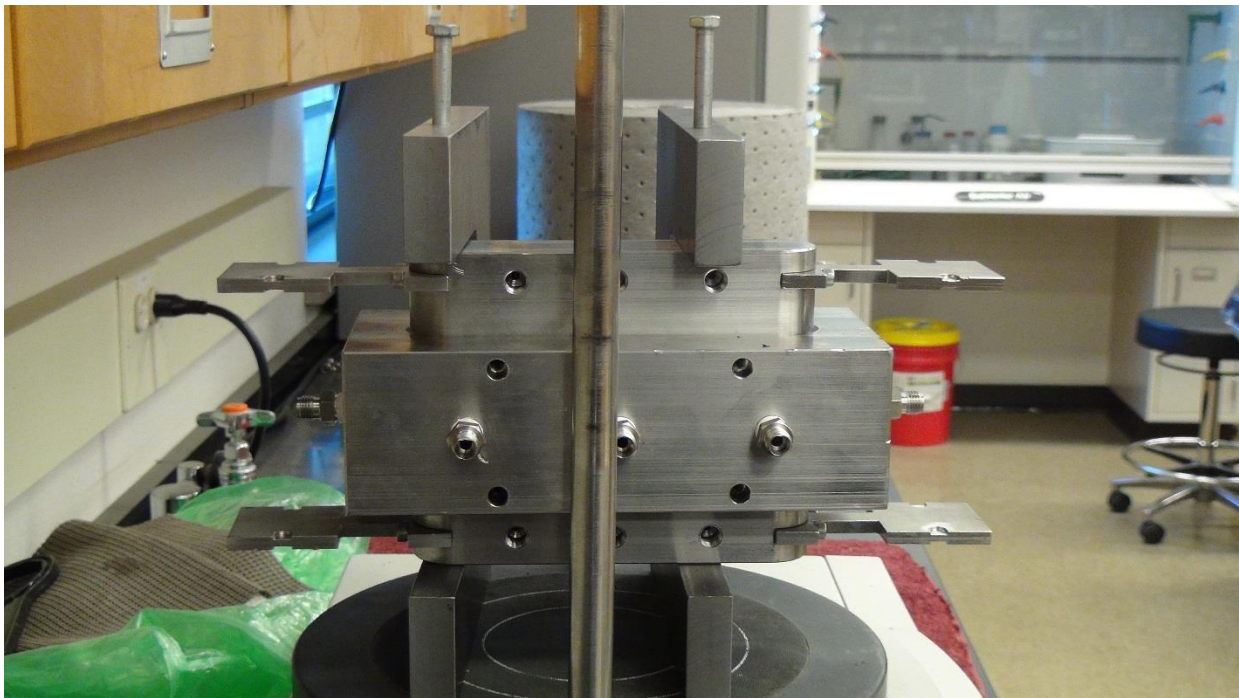


Figure 16: Loaded Cell Inside Clamps

The clamps keep the top piston static through the vibration. During the vibration stage proppant is rearranged which can cause the steel platen and top piston to lower. If the top piston is lowered the bolts on the clamps are tightened until the base of the bolts reach the top piston. This removes the ability of the top piston to move upwards during the rest of the vibration.

To produce the vibration, initially an engraving rotary tool was used. Without the ability to properly measure the vibrational amplitude exerted by the tool and no ideal location to attach the tool to the cell, this method was not considered appropriate.

The next vibration source was an AS 200 sieve shaker. The cell inside the clamp was placed on the center of the shaker vibration plate. A level was used during the vibration ensured the cell remained in the middle of the plate. If the cell was not level during vibration, proppant would migrate to the lower end and the cell would need to be repacked. The AS 200 digit used a control that can set vibration amplitude as a percentage of maximum. The maximum amplitude for this machine is 3.00 mm. Testing was conducted at various vibration amplitudes, and the results are in Table X.

Table X: Vibration Test

Amplitude (% of Max)	Proppant Movement
30	None
58	Singular proppant rearrangement
68	Entire pack moves around cell

Each of these tests were performed on cells which had been properly loaded and leveled. The top piston was not inserted so proppant movement could be monitored. At 30% of the maximum amplitude the proppant was not influenced and no movement was recorded. At 68% of the maximum amplitude all the proppant in the cell violently moved around the cell and proppant began to bounce out of the cell. At 58% of the maximum amplitude the proppant

movement was reduced to singular grains being displaced inside the pack which is the ideal effect. This small rearrangement creates the tighter packs and reduces the point loading inside the cell.

An important point to note is that the AS 200 is only rated to hold 9 kg. The cells loaded with proppant and inside the clamps have a mass of 29 kg. With the system being 20 kg over the rated limit it is difficult to measure the actual vibration level that the cell experiences.

7.3.2. Cell Vibration Results

The cells were placed in the clamps and vibrated at 58% of maximum amplitude before being placed inside the load frame to be tested. Figure 17 is a graph of the average conductivities calculated using this testing procedure.

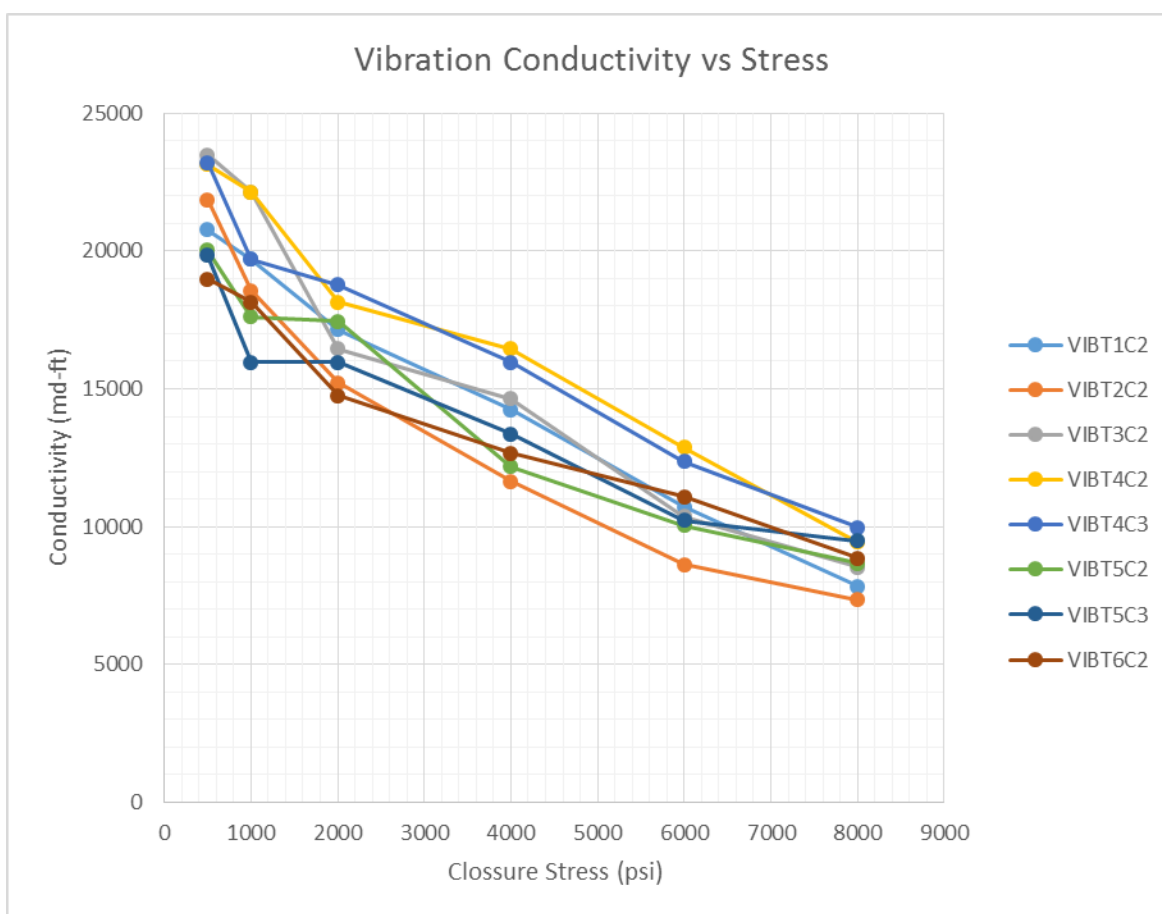


Figure 17: Vibration Conductivity Graph

The vibration process produced a very tight spread in data at the initial closure stress of 500 psi. As the stress increased the spread remained tight, with the largest spread of data occurring at 1000 psi. For every other testing procedure, the largest variance in the data was at 6000 psi. This procedure produced a tighter packs and when exposed to the 6000 psi closure stress, grain rearrangement was minimal. The most impressive result from this procedure was the small spread in data at 8000 psi. A comparison of the API standard loading procedure and vibration procedure data is shown in Table XI.

Table XI: API Standard Loading and Vibration Data

API Standard Loading Procedure				Vibration			
Closure Stress (psi)	Average Conductivity (md-ft)	Standard Deviation	Variance	Closure Stress (psi)	Average Conductivity (md-ft)	Standard Deviation	Variance
500	21,633	2507	6,285,704	500	21,416	1485	2,205,598
1000	19,811	2277	5,186,623	1000	19,248	2112	4,461,845
2000	17,700	2357	5,554,122	2000	16,740	1181	1,394,492
4000	16,214	2671	7,133,495	4000	13,893	1678	2,817,344
6000	12,915	3246	10,536,238	6000	10,784	1340	1,796,188
8000	10,208	1575	2,480,842	8000	8,768	876	767,306

This table is a good summary of how the vibration testing produces very similar average conductivities to the API standard loading procedure. The API standard procedure on average produces an average conductivity 1200 md-ft larger than the vibration testing but the API loading procedure variances were three times larger than the vibration tests. This means that the vibration tests were able to produce similar values to the API loading procedure but with less spread in the data. This point is further illustrated by the error bar conductivity comparison graph in Figure 18.

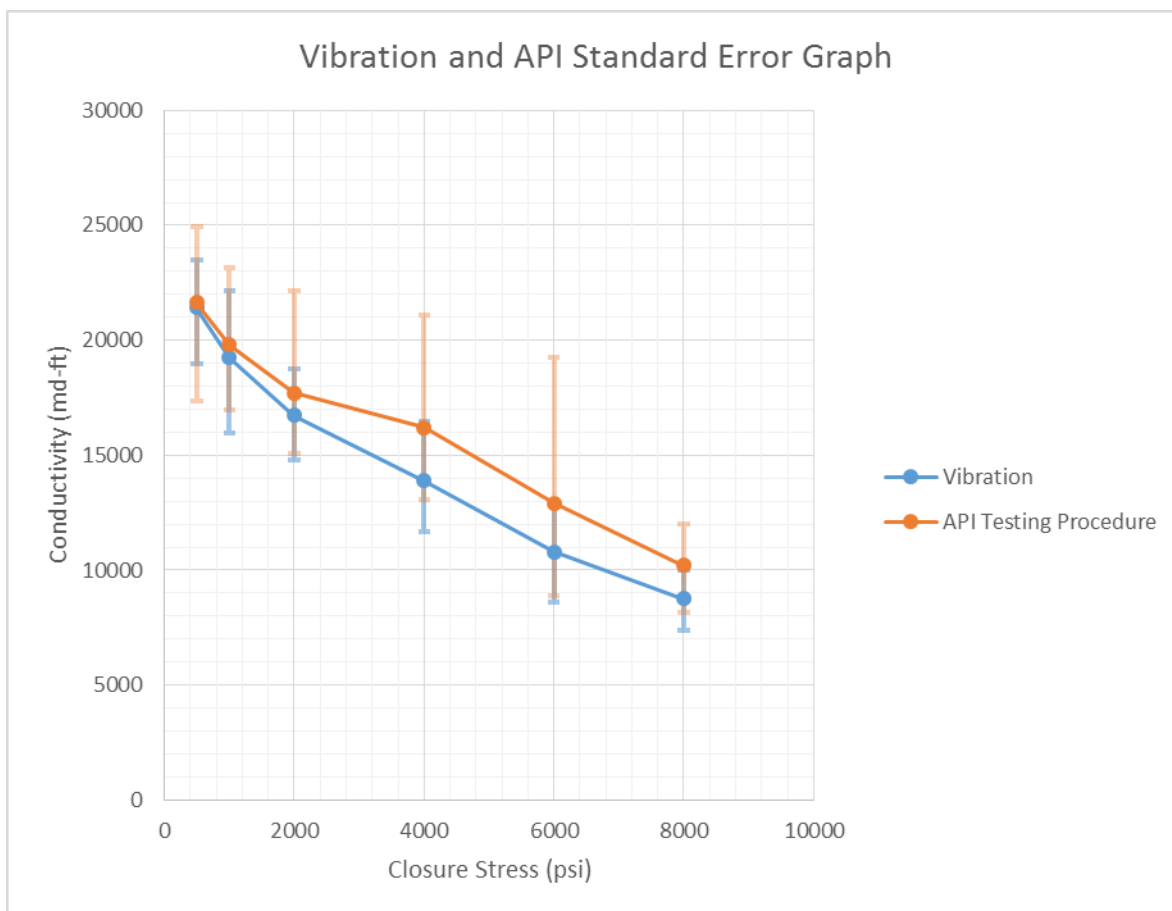


Figure 18: Vibration and API Testing Procedure Conductivity Error Graph

At 500 psi the vibration spread was considerably smaller than the API standard procedure, which was expected. The vibration should create much tighter packs for the initial stresses which experienced very little proppant rearrangement. At 1000 psi the vibration data had the largest spread in data, which is caused by the results from Test 5 Cell 3. Looking at Figure 16, at 1000 psi Test 5 Cell 3 conductivity barely changes from 1000 psi to 2000 psi closure stress. This cell had a high pack height, which indicated the vibration was unable to create an initial tight pack for that cell. For the remaining closure stresses, the vibration produced data spreads significantly lower than the API standard loading procedure.

The average conductivities produced by each test were very similar, Table XII is a comparison of the average pack widths for each of these testing procedures.

Table XII: API Standard Loading and Vibration Average Widths

API Standard Loading		Vibration	
Closure Stress (psi)	Average Width (in)	Closure Stress (psi)	Average Width (in)
500	0.2669	500	0.2671
1000	0.2629	1000	0.2632
2000	0.2580	2000	0.2583
4000	0.2520	4000	0.2517
6000	0.2447	6000	0.2459
8000	0.2354	8000	0.2365

Both of these tests generated very similar average pack widths. The vibration test on average had a higher average width by 0.0005 in. This result supports the fact that the vibration testing was producing the same findings as the API standard loading procedure except with less spread. Figure 19 is a graph of the average permeabilities from the vibration and API standard loading test.

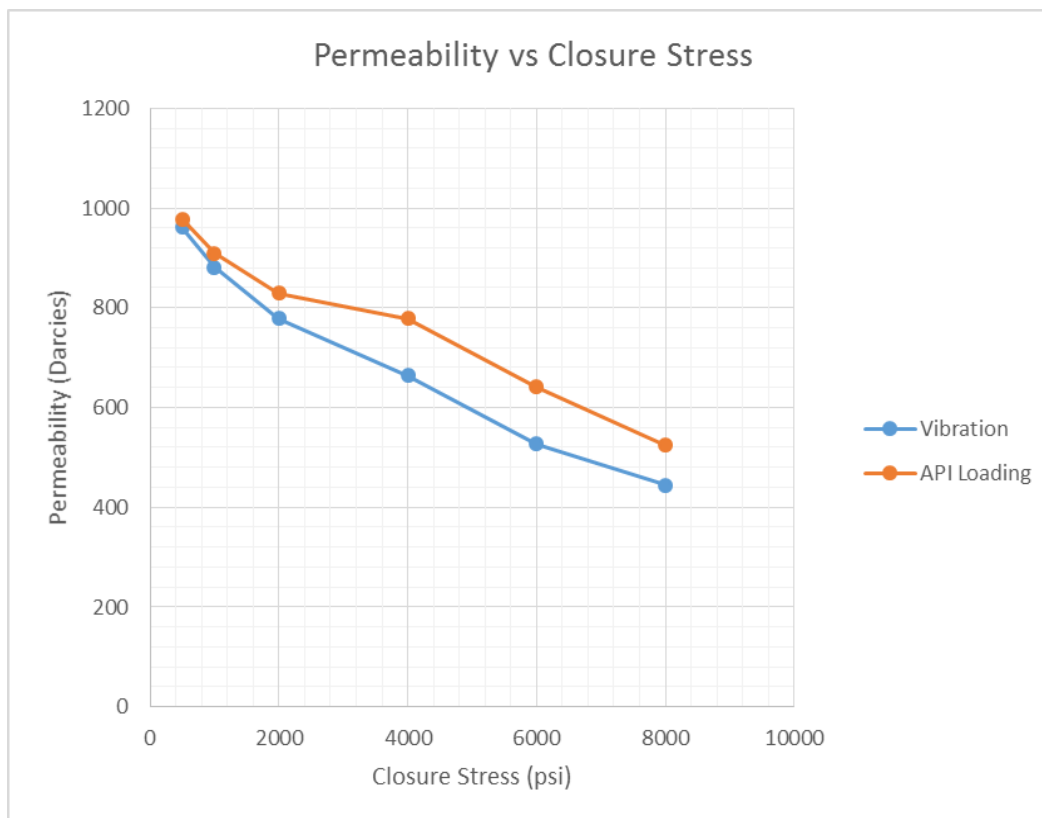


Figure 19: Vibration and API Testing Procedure Permeability Graph

From this graph it is clear that the permeabilities from the vibration tests and API loading tests generated very similar data. At the initial closure stresses, the vibration and API loading were essentially the same. The largest difference in the permeabilities was at 4000 psi and 6000 psi where the API loading procedure had the highest variance. The initial permeabilities for the two tests were almost identical, which reinforces the point that the vibration tests produce very similar results to the API loading procedure but with less variation in the data.

8. Conclusions

1. Without proper fitting sizes the Hoke cylinder injection process was not workable.
2. From the guar injection tests it was clear that using a guar polymer to aid in the injection process reduced the overall permeability of the proppant.
3. Flowing an oxidizer such as sodium pyrophosphate through the cell for a minimum period of time before again flushing the cell with 2% KCl would remove the guar from the cell and produce a better comparison for this method.
4. Vibrating loaded cells before testing generated tight proppant packs with very little grain rearrangement when exposed to various closure stresses. The resulting conductivities had less spread in the data when compared to the conductivities from the API standard loading procedure.
5. Through testing these various procedures, two mass flow controllers were used and broken. During the vibration tests the mass flow started initially at maximum flow and was only able to go to lower flow rates. This meant testing started at 8 cm³/min then 4 cm³/min and 2 cm³/min. The system was either too hot for the controllers or flowing 2% KCl was clogging the mass flow controllers.
6. Conducting more API standard loading procedure tests may reduce the variation in the data. Unfortunately, due to tubing leaks and mass flow controls not working properly, no further tests were conducted for this thesis.

9. Recommendations and Future Research

1. Purchase larger tubing and connections to test the viability of the Hoke cylinder injector.
2. Flowing proppant into cells in a slurry may give a better representation of how proppant is transported during a hydraulic fracture.
3. If testing is to continue on the effects of cell vibration for conductivity tests at Montana Tech, it is recommended that the school purchase a vibration instrument rated to the cell's weight.
4. Because the results from the vibration testing were very promising for short-term conductivity tests, more investigation into what the optimal vibrational amplitude should be to apply to a cell to achieve the lowest spread in conductivities is an area that should be further investigated.
5. Because the proposed loading procedures were evaluated in the API 61 (1989) short-term conductivity test, the next step in research progression would be to measure the effectiveness of these tests in the API-19D (2008) long-term conductivity test. The long-term test is the current industry standard for proppant testing. A reduction in variation for the long-term tests would be invaluable for industry.
6. The line leading to the mass flow controller could be lengthened giving the fluid more time to cool, or the lines could be run through a cooler before reaching the controller.
7. The two mass flow controllers in the lab need to be repaired and modified to be able to withstand higher temperatures.
8. The nylon tubing which connects the cells to the pressure transducers needs to be replaced. After numerous tests at high temperatures the tubing begins to degrade and there are leaks at the connections. Replacing the current tubing with steel tubing or nylon

tubing rated for higher temperatures would reduce the small fluctuations read by the differential pressure transducer.

9.1 Future Research

For these tests steel platens were used in substitution for the API recommended sandstone platens. The sandstone platens are a poor representation of the reservoirs typically hydraulically fractured. In a 2012 study by Texas A&M University (Zhang, et al. 2013), fracture conductivity in the Barnett Shale was investigated. To test the Barnett Shale, the original conductivity cell design was modified to fit larger platens. The new platens were 0.15 in wider and 2.65 in thicker. Figure 20 displays the shale cores used in the experiment.



Figure 20: Barnett shale samples shaped to fit into modified API conductivity cell (Zhang, et al. 2013)

The platens were harvested from a shale outcropping in central Texas, but the samples were only 1 in to 1.5 in thick. Sandstone platens were combined with the shale platens to reach the 3 in thickness requirement that the modified cell requires (the image on the right shows the sandstone and shale combination). The experiment tested short and long-term conductivity. For the long-term, a closure stress of 6000 psi was induced and held for the required 50 hours \pm 2 hours. The conductivity decreased 19% in the first 20 hours then remained unchanged for the remainder of

the test. This result indicates that shale platens can be used in conductivity tests. Further research into the effectiveness of thinner shale platens could yield important results.

References

- Anderson, R. (2013). *Performance of Fracturing Products*. Chandler: US SILICA.
- API RP 61. (1989). *Recommended Practices for Evaluating Short-term Proppant Pack Conductivity*.
- API RP-19D. (2008). *Measuring the Long-term Conductivity of Proppants*.
- Barree, R. D., Cox, S. A., Barree, V. L., & Conway, M. W. (2003). Realistic Assessment of Proppant Pack Conductivity for Material Selection. *SPE 84306*, 12.
- Mattson, E. D., Huang, H., Conway, M., & O'Connell, L. (2014). Discrete Element Modeling Results of Proppant Rearrangement in Cooke Conductivity Cell. *SPE 168604*, 9.
- Triola, M. F. (2006). *Elementary Statistics Tenth Edition*. Boston: Pearson Education Inc.
- Zhang, J., Kamenov, A., Zhu, D., & Hill, A. D. (2013). Laboratory Measurement of Hydraulic Fracture Conductivities in the Barnett Shale. *SPE 163839*, 22.

Appendix A: Conductivity Results

Summary API Standard Procedure					
Closure Stress (psi)	Average Conductivity (md-ft)	Standard Deviation	Variance	Max Conductivity (md-ft)	Min Conductivity (md-ft)
500	21,633	2,507	6,285,704	3,335	4,283
1000	19,811	2,277	5,186,623	3,330	2,830
2000	17,700	2,357	5,554,122	4,449	2,644
4000	16,214	2,671	7,133,495	4,881	3,135
6000	12,915	3,246	10,536,238	6,334	4,055
8000	10,208	1,575	2,480,842	1,784	2,070

Summary Guar Inject Test									
Closure Stress (psi)	Conductivity (md-ft)	Standard Deviation	Variance	Max Conductivity (md-ft)	Min Conductivity (md-ft)	T-Test (variance differences)	T-Test (Root)	T value	Degrees of freedom
500	17,336	1,754	3,076,297	1,883	3,208	1,337,429	1156	3.72	12
1000	15,495	1,516	2,297,338	2,059	1,973	1,069,137	1034	4.17	12
2000	14,082	1,512	2,285,321	2,094	1,706	1,119,920	1058	3.42	12
4000	11,657	2,132	4,547,537	3,250	3,544	1,668,719	1292	3.53	12
6000	8,911	2,004	4,017,986	2,820	2,790	2,079,175	1442	2.78	12
8000	6,796	1,364	1,859,794	1,695	2,674	620,091	787	4.33	12

Summary Guar Inject Set									
Closure Stress (psi)	Conductivity (md-ft)	Standard Deviation	Variance	Max Conductivity (md-ft)	Min Conductivity (md-ft)	T-Test (variance differences)	T-Test (Root)	T value	Degrees of freedom
500	11,269	1,410	1,986,911	1,407	2,293	1,229,110	1109	9.35	11
1000	11,545	1,356	1,839,742	1,240	2,217	1,047,570	1024	8.08	11
2000	10,837	1,130	1,277,179	1,436	1,977	1,006,309	1003	6.84	11
4000	8,454	1,589	2,523,691	1,972	1,887	1,439,686	1200	6.47	11
6000	5,895	2,077	4,315,884	3,277	2,607	2,224,491	1491	4.71	11
8000	5,199	2,038	4,153,955	2,939	2,223	1,046,732	1023	4.90	11

Summary Vibration Testing									
Closure Stress (psi)	Average Conductivity (md-ft)	Standard Deviation	Variance	Max Conductivity	Min Conductivity	T-Test (variance differences)	T-Test (Root)	T value	Degrees of freedom
500	21,416	1485	2,205,598	2075	2,431	1,173,657	1083	0.20	13
1000	19,248	2112	4,461,845	2902	3,287	1,298,677	1140	0.49	13
2000	16,740	1181	1,394,492	2027	1,973	967,758	984	0.98	13
4000	13,893	1678	2,817,344	2551	2,244	1,371,239	1171	1.98	13
6000	10,784	1340	1,796,188	2083	2,160	1,729,700	1315	1.62	13
8000	8,768	876	767,306	1202	1,419	450,319	671	2.15	13

Appendix B: Raw Data

API Conductivity Testing Results

2nd Baseline Test Cell 2			5th Baseline Test Cell 3			6th Baseline Test Cell 2			7th Baseline Test Cell 3		
Closure Stress (psi)	Conductivity (md-ft)	Conductivity (d-cm)	Closure Stress (psi)	Conductivity (md-ft)	Conductivity (d-cm)	Closure Stress (psi)	Conductivity (md-ft)	Conductivity (d-cm)	Closure Stress (psi)	Conductivity (md-ft)	Conductivity (d-cm)
500	24,968	761	500	17,350	529	500	22,470	685	500	23,492	716
1000	23,142	705	1,000	16,981	518	1,000	21,286	649	1,000	21,581	658
2000	22,149	675	2,000	15,056	459	2,000	17,637	538	2,000	17,077	521
4000	21,095	643	4,000	13,079	399	4,000	16,791	512	4,000	14,766	450
6000	19,249	587	6,000	8,860	270	6,000	12,465	380	6,000	10,791	329
8000	11,992	366	8,000	8,263	252	8,000	9,493	289	8,000	8,138	248

8th Baseline Test Cell 2			9th Baseline Test Cell 2			9th Baseline Test Cell 3		
Closure Stress (psi)	Conductivity (md-ft)	Conductivity (d-cm)	Closure Stress (psi)	Conductivity (md-ft)	Conductivity (d-cm)	Closure Stress (psi)	Conductivity (md-ft)	Conductivity (d-cm)
500	22,149	675	500	21,296	649	500	19,706	601
1000	18,563	566	1000	19,570	596	1000	17,554	535
2000	18,141	553	2000	18,458	563	2000	15,381	469
4000	16,612	506	4000	17,275	527	4000	13,882	423
6000	13,756	419	6000	13,379	408	6000	11,906	363
8000	11,075	338	8000	10,927	333	8000	11,571	353

Guar Injection Data

Guar Inject Test 1 Cell 2			Guar Injection Test 1 Cell 3			Guar Injection Test 2 Cell 3			Guar Inject Test 3 Cell 3		
Closure Stress (psi)	Conductivity (d-cm)	Conductivity (md-ft)	Closure Stress (psi)	Conductivity (d-cm)	Conductivity (md-ft)	Closure Stress (psi)	Conductivity (d-cm)	Conductivity (md-ft)	Closure Stress (psi)	Conductivity (d-cm)	Conductivity (md-ft)
500	512	16791	500	431	14129	500	585	19196	500	523	17160
1,000	506	16612	1,000	419	13756	1,000	487	15970	1,000	412	13523
2,000	493	16175	2,000	416	13636	2,000	411	13473	2,000	377	12376
4,000	454	14907	4,000	380	12465	4,000	389	12757	4,000	368	12059
6,000	358	11731	6,000	340	11153	6,000	267	8764	6,000	254	8343
8,000	223	7317	8,000	259	8491	8,000	224	7349	8,000	197	6459

Guar Inject Test 4 Cell 3			Guar Inject Test 8 Cell 2			Guar Inject Test 9 Cell 2		
Closure Stress (psi)	Conductivity (d-cm)	Conductivity (md-ft)	Closure Stress (psi)	Conductivity (d-cm)	Conductivity (md-ft)	Closure Stress (psi)	Conductivity (d-cm)	Conductivity (md-ft)
500	586	19220	500	551	18068	500	512	16791
1,000	535	17554	1,000	450	14766	1,000	496	16286
2,000	389	12779	2,000	427	14015	2,000	491	16118
4,000	318	10426	4,000	247	8113	4,000	331	10869
6,000	219	7187	6,000	187	6121	6,000	277	9077
8,000	197	6459	8,000	126	4122	8,000	225	7373

Residual Guar Data

Guar Inject Test 4 Cell 2 (set)			Guar Inject Test 5 Cell 2 (set)			Guar Inject Test 5 Cell 3 (set)			Guar Inject Test 6 Cell 3 (set)		
Closure	Conductivity	Conductivity	Closure	Conductivity	Conductivity	Closure	Conductivity	Conductivity	Closure	Conductivity	Conductivity
500	386	12676	500	380	12465	500	313	10261	500	356	11665
1,000	377	12367	1,000	390	12784	1,000	386	12665	1,000	324	10643
2,000	331	10869	2,000	347	11372	2,000	374	12273	2,000	322	10574
4,000	200	6567	4,000	213	6977	4,000	318	10426	4,000	284	9328
6,000	100	3289	6,000	134	4406	6,000	280	9173	6,000	208	6818
8,000	223	7317	8,000	91	2976	8,000	248	8138	8,000	132	4321

Guar Inject Test 7 Cell 2 (set)			Guar Inject Test 8 Cell 3 (set)		
Closure	Conductivity	Conductivity	Closure	Conductivity	Conductivity
500	353	11571	500	274	8975
1,000	350	11481	1,000	284	9328
2,000	338	11075	2,000	270	8860
4,000	297	9736	4,000	234	7691
6,000	199	6539	6,000	157	5147
8,000	126	4122	8,000	132	4321

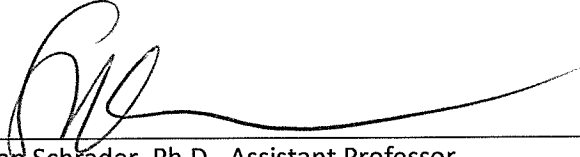
Vibration Data

Vibration Test 1 Cell 2			Vibration Test 2 Cell 2			Vibration Test 3 Cell 2			Vibration Test 4 Cell 2		
Closure Stress (psi)	Conductivity (d-cm)	Conductivity (md-ft)	Closure Stress (psi)	Conductivity (d-cm)	Conductivity (md-ft)	Closure Stress (psi)	Conductivity (d-cm)	Conductivity (md-ft)	Closure Stress (psi)	Conductivity (d-cm)	Conductivity (md-ft)
500	633	20,761	500	666	21,854	500	716	23,492	500	705	23,142
1,000	601	19,706	1,000	566	18,563	1,000	675	22,149	1,000	675	22,149
2,000	523	17,160	2,000	464	15,214	2,000	502	16,462	2,000	553	18,141
4,000	434	14,248	4,000	355	11,649	4,000	446	14,630	4,000	501	16,444
6,000	326	10,710	6,000	263	8,624	6,000	316	10,359	6,000	392	12,868
8,000	239	7,831	8,000	224	7,349	8,000	260	8,537	8,000	288	9,437

Vibration Test 4 Cell 3			Vibration Test 5 Cell 2			Vibration Test 5 Cell 3			Vibration Test 6 Cell 2		
Closure Stress (psi)	Conductivity (d-cm)	Conductivity (md-ft)	Closure Stress (psi)	Conductivity (d-cm)	Conductivity (md-ft)	Closure Stress (psi)	Conductivity (d-cm)	Conductivity (md-ft)	Closure Stress (psi)	Conductivity (d-cm)	Conductivity (md-ft)
500	707	23,204	500	611	20,040	500	605	19,852	500	579	18,985
1,000	601	19,706	1,000	537	17,604	1,000	486	15,961	1,000	553	18,141
2,000	572	18,767	2,000	532	17,446	2,000	407	15,961	2,000	450	14,766
4,000	486	15,961	4,000	371	12,175	4,000	486	13,360	4,000	386	12,676
6,000	377	12,367	6,000	306	10,037	6,000	312	10,223	6,000	338	11,087
8,000	304	9,970	8,000	264	8,669	8,000	289	9,493	8,000	270	8,860

SIGNATURE PAGE

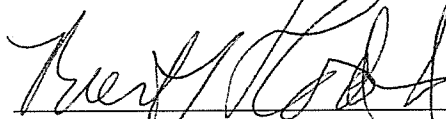
This is to certify that the thesis prepared by Kent Blair entitled "Modifying Fracture Conductivity Testing Procedures" has been examined and approved for acceptance by the Department of Petroleum Engineering, Montana Tech of The University of Montana, on this 2nd day of December, 2015.



Susan Schrader, Ph.D., Assistant Professor
Department of Petroleum Engineering
Chair, Examination Committee



Richard Schrader, Lab Director/Instructor
Department of Petroleum Engineering
Member, Examination Committee



Burt Todd, Ph.D., Department Head
Department of Petroleum Engineering
Member, Examination Committee



Paul Conrad, Ph.D., Professor
Department of Mining Engineering
Member, Examination Committee



Brandon DeShaw
Global Energy Laboratories
Member, Examination Committee